GA-A15953

MASTER

RADIATION SHIELDING DESIGN CONSIDERATIONS FOR DOUBLET III

by
B. A. ENGHOLM

JUNE 1980

GENERAL ATOMIC COMPANY

DISCLAIMER

DISCLAIMER

Master

CONF-800607--86

GA-A15953

RADIATION SHIELDING DESIGN CONSIDERATIONS FOR DOUBLET III

by

B. A. ENGHOLM

An oral version of this paper was presented at the American Nuclear Society 1980 Annual Meeting, Las Vegas, Nevada, June 9-12, 1980.

Work supported by
Department of Energy
Contract DE-AT03-76ET51011

GENERAL ATOMIC PROJECT 3235.803.454
JUNE 1980

GENERAL ATOMIC COMPANY

CONTENTS

FIGURES

TABLES

1. SUMMARY

Calculations and measurements were made of the bremsstrahlung (X-ray) doses resulting from runaway electron shots at Doublet III. The analysis considered direct, wall-scattered, and skyshine contributions. Reasonably good agreement was obtained between calculations and measurements. The X-ray dose in the control room was about 1 mR per runaway shot, while that at the north boundary was undetectable, with a calculated value of 0.05 mR per shot. These low doses attest to the adequacy of the 2 ft concrete shadow shield surrounding the Doublet III room.

Exploratory shielding analyses were performed for possible neutron generation if Doublet III were operated with neutral beam injection in an aggressive D-D mode. These calculations assisted in planning for the DIII Upgrade Program. General conclusions were that the existing concrete shield walls would have to be extended and increased to 3 or 4 ft in thickness, and that a shield roof would have to be installed to control skyshine. The shield roof thickness would be about a foot less than the wall thickness. Several streaming pathways were investigated and solutions suggested.

2. INTRODUCTION

The Doublet III experiment at General Atomic is part of DOE's long-range fusion development program. Startup of Doublet III took place in February 1978, and during 1978 and 1979 the machine was operated with ohmic discharges and various plasma configurations (doublets and dees). Plasma densities of 10^{14} cm^{-3} and plasma currents of 2 MA have been achieved. During 1981, two neutral beam injectors are being installed, leading to operation at 7.2 MW by late 1981. The ultimate goal is to demonstrate the advantages of noncircular shape at near breakeven plasma parameters[1].

In 1977, the Doublet III Project desired to confirm the adequacy of their concrete wall shadow shield design to protect the working personnel and the public from bremsstrahlung radiation resulting from runaway electron shots. The cooperation of C. L. Hsieh, J. F. Baur, and R. P. Seraydarian enabled this author to compile the information in Section 3 of this report; and Safety Engineer J. D. Jones' recent measurements provided an interesting comparison with the calculations.

In 1979, when plans for the Doublet III Upgrade were being formulated and neutral beam injection scenarios evaluated, D. H. Service and E. L. Hubbard of the Doublet III Project requested studies of the additional shielding needed for possible D-D neutron operation of DIII. Some preliminary calculations in this area had already been performed by T. J. Woods, but they needed to be expanded and refined. In this area of work, the author obtained valuable assistance from E. T. Cheng, J. Hildebrand, Jr., and S. G. Visser. The problem turned out to be remarkably similar to the PDX upgrade study performed for Princeton by EG&G/Idaho[2]. The methods and results of the Doublet III study are reported in Section 4 of this document.

3. BREMSSTRAHLUNG SHIELDING ANALYSIS

Shielding for non-beamline operation of Doublet III is provided to attenuate bremsstrahlung radiation (X-rays) to acceptable levels in the control room at the site boundary. Bremsstrahlung radiation arises from stray or runaway electrons striking the vacuum wall and/or the limiter. This phenomenon is well known, and is also observed in PLT, TFR, T-10, and other experimental fusion devices.

The bremsstrahlung shielding analysis for Doublet III was performed in 1977, followed by measurements in 1978 and 1979. A detailed description is given below.

3.1. SOURCE TERMS

3.1.1. Intensities

In a study[3] of runaway discharges in Doublet III, C. L. Hsieh calculated a maximum runaway current of 0.5 megamp, integrating 5×10^{16} electrons per shot of 2 MeV energy*. A comparison with PLT experience[5] is shown in Table 1.

TABLE 1
D-III PREDICTIONS VS PLT EXPERIENCE

	D-III	PLT
Runaway Current (megamp)	0.5	0.5
Pulse Length (sec)	0.5	0.5
2 MeV Electrons Per Shot	5×10^{16}	6×10^{16}
Other Electrons	None Assumed	Energies up to 10 MeV

*The assumption of a monoenergetic source at 2 MeV rather than an entire spectrum up to 10 MeV was shown to be valid in a recent ORNL paper[4].

A further assumption was made that one-half of the runaway electrons hit the limiter and the other half hit the Inconel vacuum chamber wall. At the time the study was performed, the limiter material was 90% Ta, 10% W, with a Z of 73. The limiter material was later changed to Inconel, with an equivalent Z of 27. The results for a tantalum limiter can easily be adjusted to Inconel for subsequent comparison with measurements.

Conversion efficiency of electrons to bremsstrahlung was calculated from the formula adapted from page 76 of Ref. 6:

$$w = \frac{0.04\ (E + 1)\ Z}{1 + 0.15\ \ln \frac{82}{Z}}$$

some results of which are listed below.

TABLE 2
ELECTRON-TO-X-RAY CONVERSION EFFICIENCIES

Electron Energy, E (MeV)	Z = 27	Z = 73
1	1.8%	5.0%
2	2.8	7.5
3	3.7	10.0
5	5.5	15.0
10	10.0	27.0

For conservatism, the conversion efficiency was taken as 3% in Inconel and 8% in tantalum, yielding 0.75×10^{15} MeV per shot from the wall and 2×10^{15} MeV per shot from a tantalum limiter.

3.1.2. Spectra

The X-ray energy spectrum can be estimated from Fig. 2.11.9(a) of Ref. 6, reproduced here as Fig. 1. This graph depicts the bremsstrahlung

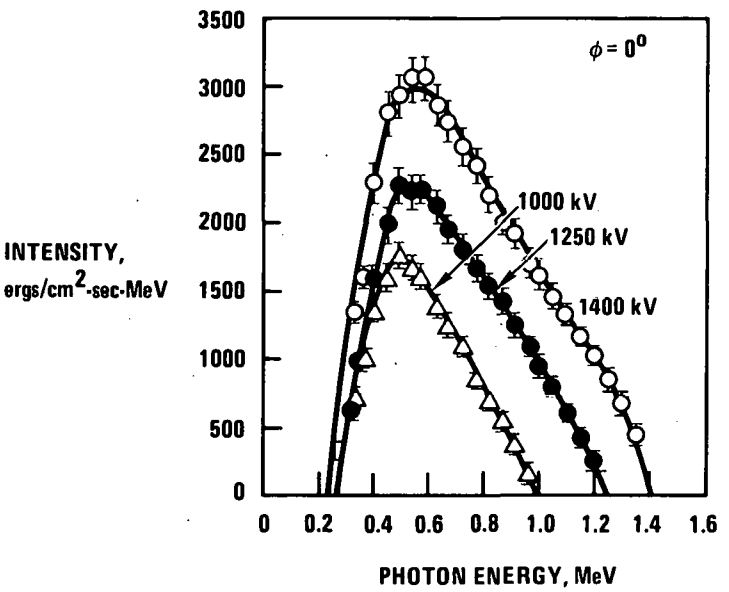

Fig. 1. Bremsstrahlung spectra in forward direction

spectra resulting from a beam of electrons stopped by a tungsten target. It will be observed that as the electron energy is increased from 1 MeV to 1.25 MeV to 1.4 MeV, the photon spectrum hardly changes. This observation is in accord with the statement on page 76 of Ref. 6: "The spectral distribution of thick-target bremsstrahlung is roughly independent of the atomic number of the absorber and the energy of the electron." The peaks in the photon energy distributions occur at 0.5, 0.53, and 0.57 MeV, respectively, indicating that for an electron energy of 2 MeV the photon peak might occur around 0.7 MeV.

Furthermore, the shapes of the curves seem to be similar, only their absolute magnitude displaying much variation. If half the emitted photon energy is assumed to occur at 0.7 MeV the remainder can be assigned a photon energy of around 1 MeV.

3.1.3. Angular Distribution

In shielding problems that are highly direction-dependent such as in the case of Doublet III, the angular distribution of X-ray emission from the machine is one of the most important input parameters. In general, the X-ray angular distributions are highly peaked in the same direction as the stopped electron beam. Buechner (Ref. 7) did considerable work in this area, and Figs. 2a and 2b show his results for copper and tungsten targets (which may be taken equivalent to Inconel and tantalum, respectively). These graphs purport to give the bremsstrahlung intensity in R/min-mA at 1 meter, as a function of electron energy and angle of beam direction.

Buechner integrated these curves over solid angle to produce the set of curves shown in Fig. 3. For example, the integrated intensity for tungsten and an electron energy of 2 MeV is $\sim$ 1800 R/min-mA. This figure should be divided by 2π to obtain the intensity in any direction for an isotropic angular distribution, suitable for direct comparison with Fig. 2b. This quotient is 286 R/min-mA at 1m.

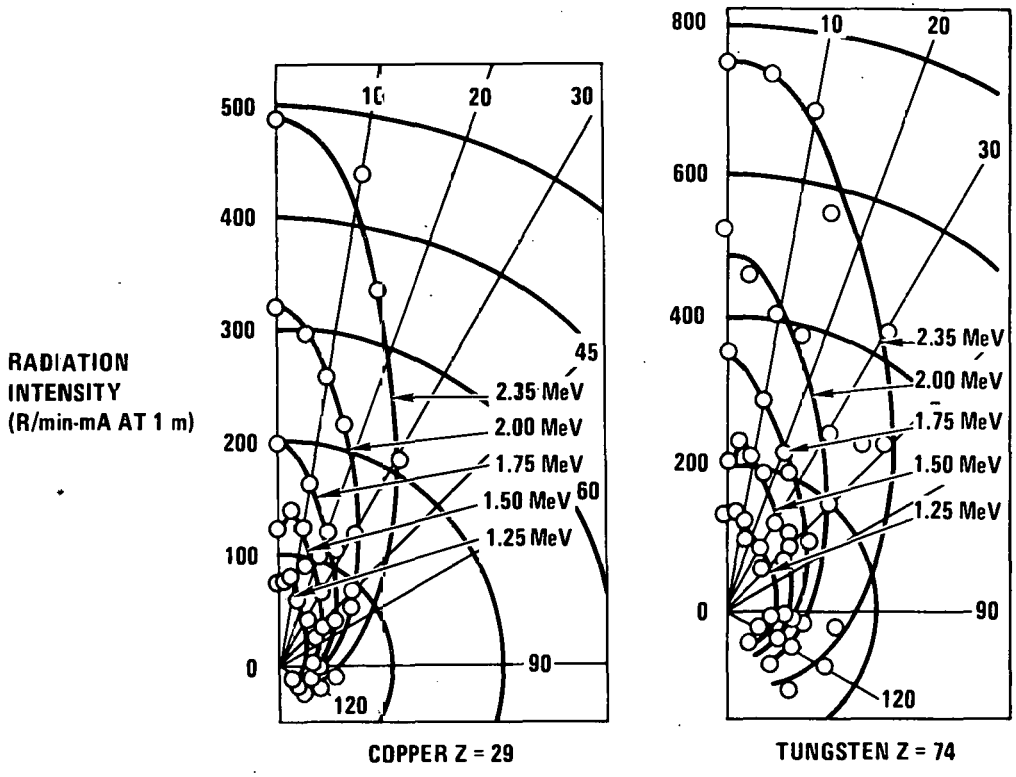

Figs. 2a and 2b. X-ray intensity at various voltages as function of angle

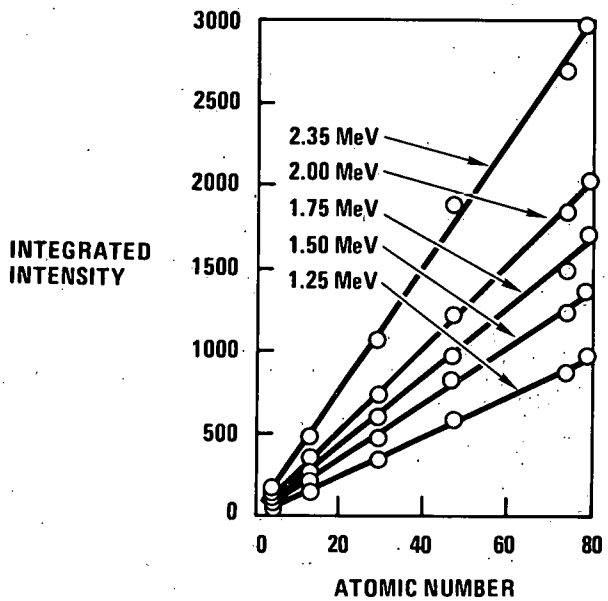

Fig. 3. Integrated X-ray intensity as a function of atomic number of target

Figure 2b shows an intensity of 480 R/min-mA in the forward (0°) direction for an electron energy of 2 MeV. Hence, there is preferential emission in the 0° direction by a factor of 480/286 = 1.67. If a direct dose rate in the 0° direction is calculated assuming an isotropic point source, the result should be multiplied by the preferential emission factor of 1.67 to obtain the true dose rate. The intensity at 25° is approximately equal to the isotropic value. Table 3 gives a list of preferential emission factors for a tungsten target.

TABLE 3
PREFERENTIAL EMISSION FACTORS FOR
ANGULAR DISTRIBUTION OF TUNGSTEN BREMSSTRAHLUNG

(Electron energy = 2 MeV)

Angle from Forward Direction	Factor
0°	1.67
10°	1.48
20°	1.13
30°	0.94
45°	0.70
50°	0.49
90°	0.38

In the case of the Inconel vacuum tank wall, runaway electrons may strike the Inconel anywhere around the circumference of the tank. Hence, the angular peaking will be apparent in an elevation view (i.e., azimuthally), but emission in the plan view (polar) will appear isotropic. Therefore, the preferential emission factors in forward directions must be reduced to account for the much larger solid angle involved (see sketches in Fig. 4). The result is a preferential emission factor of 2.05 at 0° (instead of 2.70). The other values are given in Fig. 4.

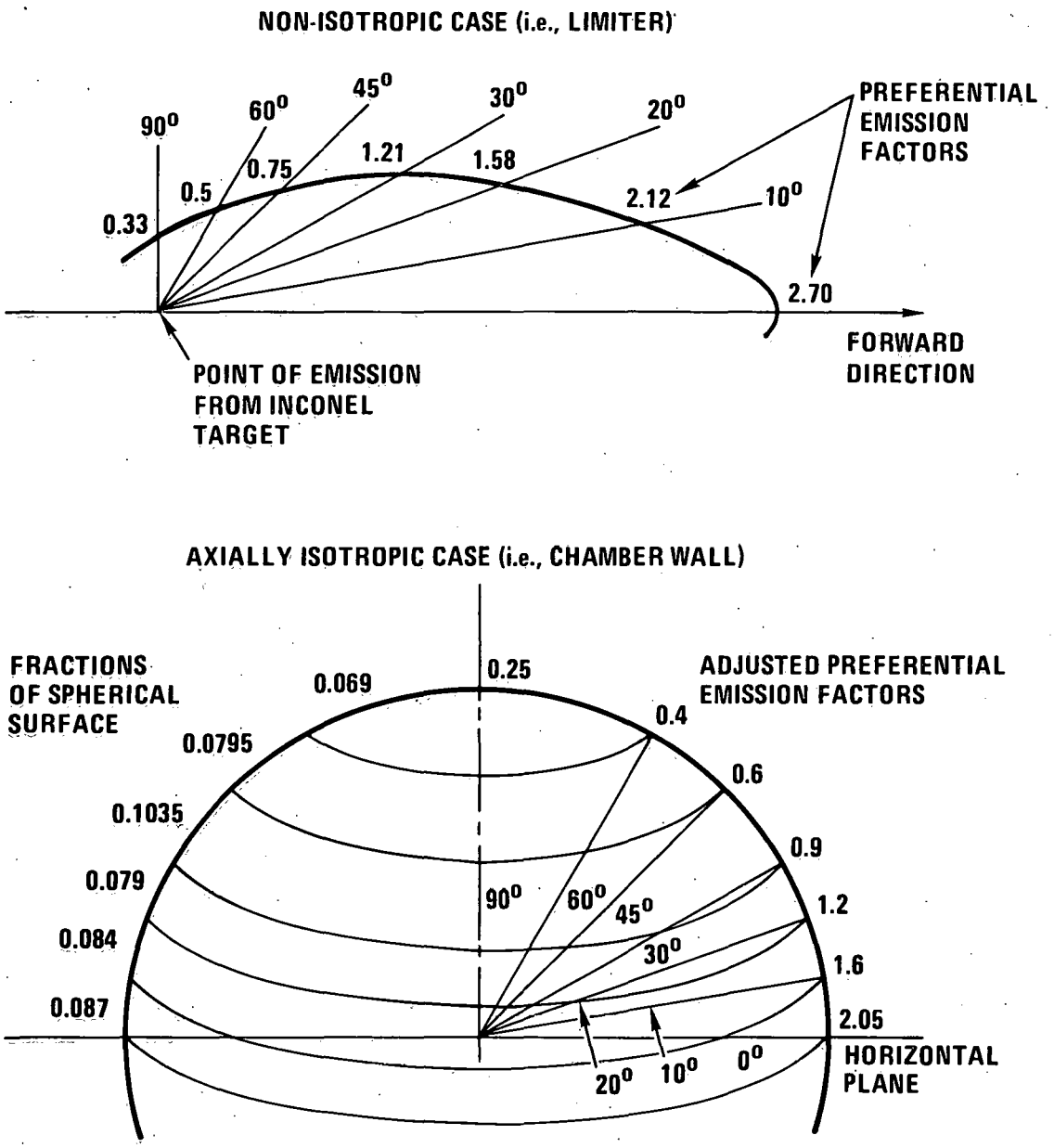

Fig. 4. Derivation of inconel preferential emission factors

The shielding effect of the copper B-coils surrounding the machine was taken as a factor of 2 reduction based on area fraction. Near the top of the machine the coils converge and a steel structural plate is installed; hence, attenuation in the 60°-90° region should be greater than a factor of 2.

3.2. GEOMETRY

Figure 5 shows an elevation of the machine envelope and the 2-ft concrete shield walls as they existed at the time of the calculation.

The location of an equivalent point source of bremsstrahlung leaving the machine could be taken at the center of the machine or somewhere on the envelope. As shown in Fig. 5, if the source point is taken at the top of the machine, the 8-ft-high shield walls subtend an angle of approximately 10° above the horizontal. If the source is taken at the geometric center of the machine, the subtended angle is 17.35°, according to a calculation by R. P. Seraydarian of the Doublet III project.

Detector locations of interest are: (a) the control room, particularly the point of maximum dose within a six-foot height; (b) the guard station, which is 240 ft from Doublet III; and (c) Dunhill Street, 280 ft away, which is just outside the site boundary.

3.3. DIRECT DOSES

The geometry and detector locations for the direct dose calculations are shown in Fig. 6. For this calculation, the source point and detectors are assumed to be at the same elevation. The concrete shield wall is 2 ft thick and has a density of 140 lb/ft^3.

Simple point-kernel attenuation theory was used:

$$D + S_\infty = \frac{C\ B\ P\ Q\ e^{-\mu t}}{4\pi\ R^2}$$

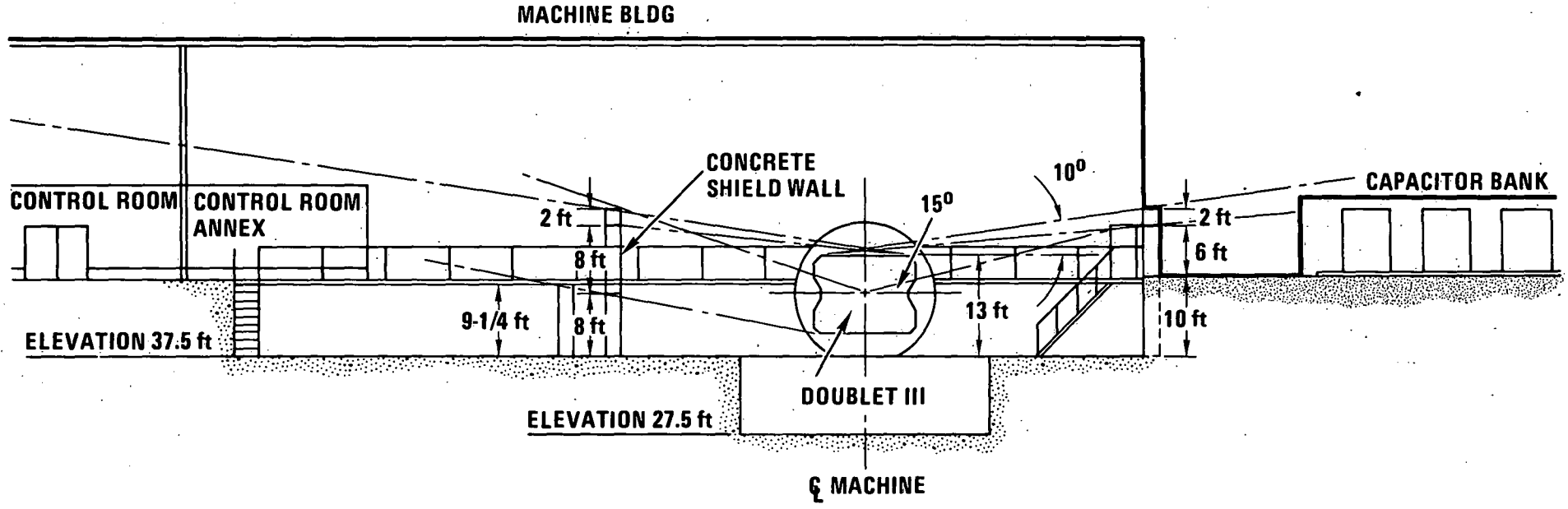

Fig. 5. Elevation view of D-III looking northwest

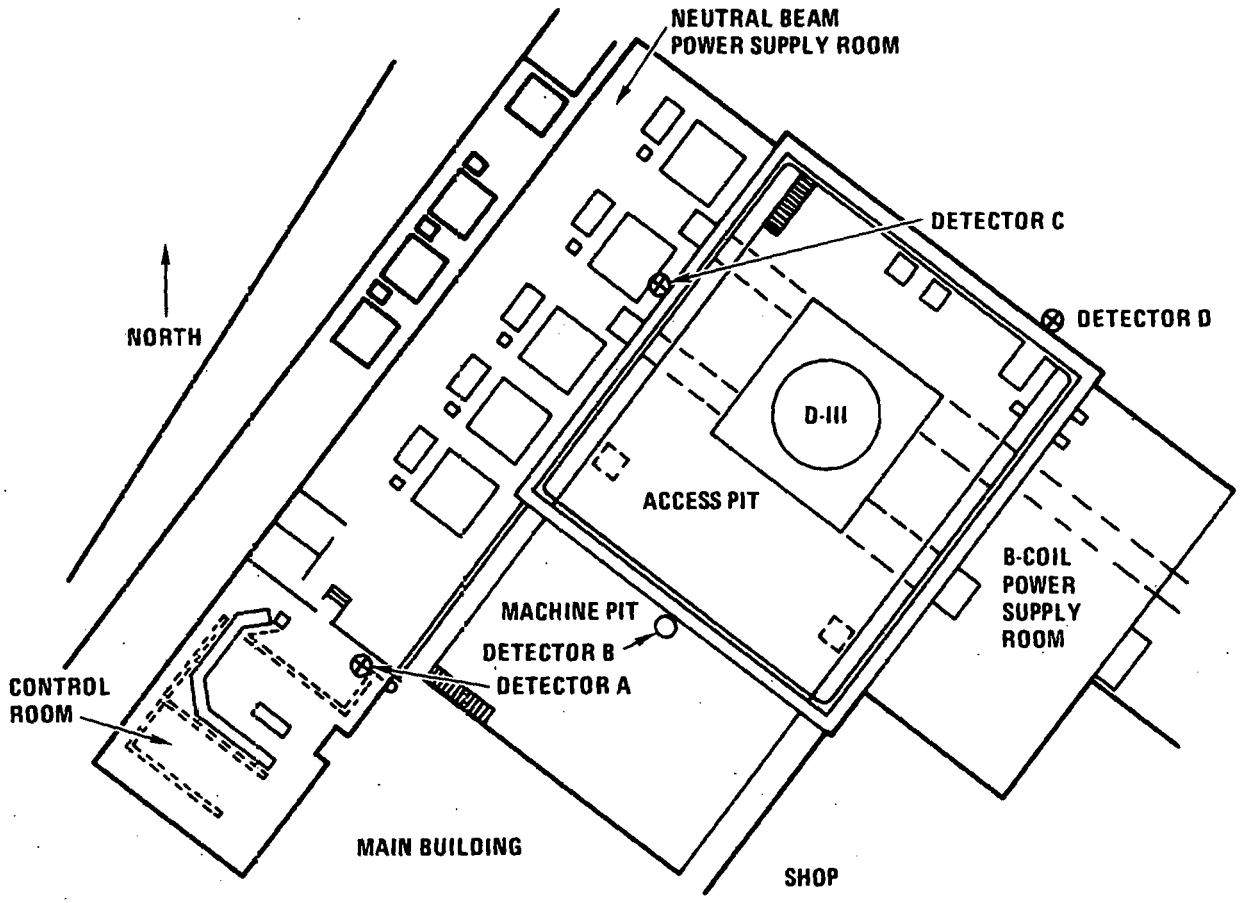

Fig. 6. Direct dose points

where $D + S_\infty$ is the uncollided plus collided gamma dose (mR)

C is the flux-to-dose conversion factor = 4.8 (-7) mR per MeV/cm^2 = 5.2 (-10) mR per MeV/ft^2

B_∞ is the buildup factor

P is the preferential emission factor

Q is the total MeV emitted (corrected for coil attenuation)

μ is the linear absorption coefficient for concrete = 0.158 cm^{-1} = 4.82 ft^{-1}

t is the line-of-sight shield thickness in ft

R is the source-detector distance in ft

Some allowance should also be made for ground scattering, which may be a 10% effect. Results are shown in Table 4.

TABLE 4
DIRECT DOSE CALCULATIONS

Detector No.	Q (MeV)	P	R (ft)	t (ft)	$e^{-\mu t}$	B_∞	$D + S_\infty$* (mR/shot)
A	0.75 (+15)	2.05	100	2.2	2.5 (-5)	26	0.004
B	0.75 (+15)	2.05	50	2.0	6.8 (-5)	22	0.042
C	0.75 (+15)	2.05	40	2.0	6.8 (-5)	22	0.064
D	** 0.75 (+15) / 2.0 (+15)	2.05 / 1.67	45	2.8	1.44 (-6)	38	0.006
	*** 0.75 (+15) / 0.75 (+15)	2.05 / 2.70	45	2.8	1.44 (-6)	38	0.0044

*Includes factor of 1.1 for ground scattering.
**Tantalum limiter.
***Inconel limiter.

Because the direct dose varies inversely as R^2, it is obvious that the direct doses at the guard station (R = 240 ft) and on Dunhill Street (R = 280 ft) will be completely negligible.

It is also clear that the 2-ft thickness of concrete is quite adequate, even for occupancy of the neutral beam power supply room.

3.4. WALL AND CEILING SCATTERED DOSES

Calculations of the wall and ceiling scattered doses were performed using the GGG-F Code[8], which computes single photon scattering from an isotropic point source to yield output with and without buildup on the scattered leg.

The geometry used for these calculations is shown in Fig. 7. Most of the computer runs were made with the detector points in the control room. The sketch shows two walls - Wall No. 1 (the long wall) and Wall No. 2 (the side wall of the control room) - and the ceiling or roof. The code can treat only one of these scattering surfaces at a time, so numerous runs had to be made.

All GGG runs were made for a unit point isotropic source strength of 1 MeV, comprised of half of a 1 MeV photon and seven-tenths of a 0.7 MeV photon. The results were later adjusted to the proper source strength and preferential emission.

The walls were assumed to extend from the top of the concrete shield (at 8 ft elevation) to the ceiling (at 28 ft elevation). The ceiling was started 30 ft away from the point source to represent the shielding offered by the copper coils and steel structure above the machine.

As an intervening scattering surface, such as Wall No. 1, is increased in thickness, the scattering rate per unit area increases, but so does the attenuation through the wall. Since the latter increases exponentially,

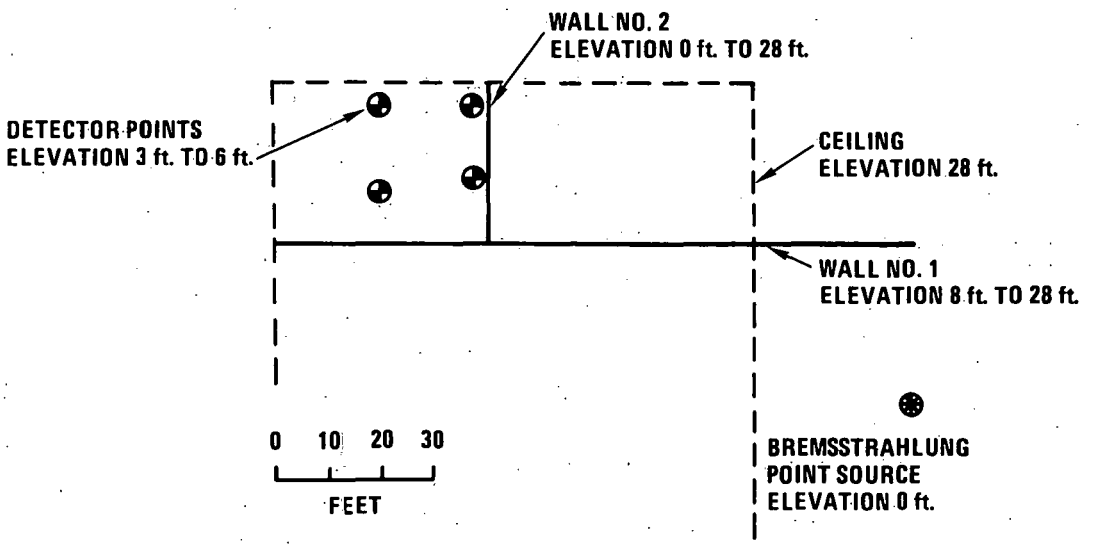

Fig. 7. Geometry for wall and ceiling scattering

there is some wall thickness which produces a maximum scattered dose on the detector side. In order to account for this effect, two different wall/ceiling thicknesses were run:

Composition A	3.945 g/cm^2 Fe
	3.945 g/cm^2 SiO_2
Composition B	7.89 g/cm^2 Fe
	3.945 g/cm^2 SiO_2

The SiO_2 is an attempt to represent insulation and/or plasterboard. The ceiling and both walls were treated as shield regions in all runs, even though only one at a time was treated as a scatterer.

After the GGG runs were completed, the results were normalized as mentioned above. Only bremsstrahlung from the vacuum chamber wall were considered, as the limiter X-ray beam is in a direction opposite from the control room and would have to scatter 180° to reach that area. As shown in Table 4, the equivalent source strength is 0.75 (+15) MeV per shot.

The preferential emission factor is estimated by observing that the source-to-wall paths generally make angles of 10° to 30° with the horizontal. Referring to Fig. 4, a factor of 1.2 looks appropriate. Hence, the source strength becomes 0.9 (+15) MeV per shot. The resulting doses are given in Table 5.

3.5. SKYSHINE DOSES

Two methods were employed in the calculation of bremsstrahlung skyshine doses from Doublet III. In both cases, attenuation by non-shielding walls and the ceiling was neglected, a conservative assumption. It was also assumed that source and detectors are all at the same elevation.

TABLE 5
WALL AND CEILING SCATTERED DOSES

	Composition A		Composition B	
	Minimum Buildup*	Maximum Buildup*	Minimum Buildup*	Maximum Buildup*
Control Room Doses (mR/shot)				
From Wall #1	0.084	0.20	0.052	0.166
From Wall #2	0.078	0.084	0.072	0.094
From Ceiling	0.012	0.064	0.010	0.052
Totals	0.174	0.348	0.124	0.312
Guard Shack Dose (mR/shot)**				
From Wall #1	0.015			
From Wall #2	0.0062 (est.)			
From Ceiling	0.0048 (est.)			
Total	0.026			
Dunhill Street Dose (mR/shot)**	0.02 (est.)			

*i.e., without or with buildup on scattered leg. For conservatism, the "Maximum Buildup" cases should be used.

**Includes air attenuation by a factor of 1.6.

3.5.1. Skyshine Method I

This method, described in Ref. 9, utilizes the formula

$$S_{sky} = K'_s \, S_\infty/2$$

where

S_{sky} is the skyshine gamma dose rate
K'_s is the skyshine correction factor shown in Fig. 8a
S_∞ is the collided direct dose rate

To obtain S_∞ one uses the recipe

$$S_\infty = (B_\infty - 1) \, D$$

where

B_∞ is the buildup factor in air
and D is the uncollided direct dose rate.

Another factor which can be injected is a skyshine angular response, $G(\omega)$, plotted in Fig. 8b. Technically, the curves are for the detector in a circular pit which reduces the solid angle subtended by the sky. The assumption will be made that the curves are equally applicable to the source in a pit. Two cases will be considered: 10° shadowing by the 8-ft-high concrete shield, and 17.35° shadowing.

With respect to the source term, it seems clear that only the vacuum chamber wall source should be used for the control room and guard shack doses, as the limiter bremsstrahlung beam heads in the opposite direction. However, some contribution from the limiter should be included in the Dunhill Street skyshine dose. Method II will attempt to treat this contribution.

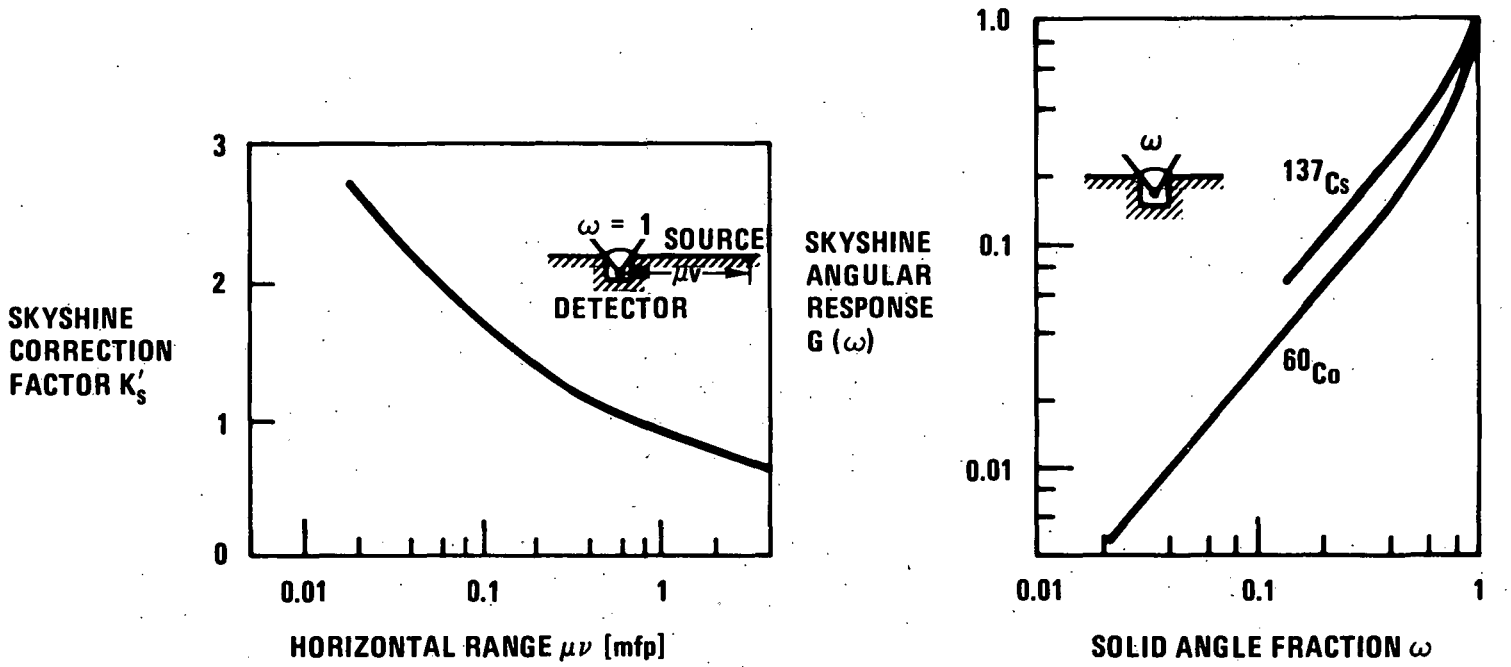

Figs. 8a and 8b. Skyshine correction factors

The mass attenuation coefficient for air will taken as 0.07 cm^2/g, giving a linear attenuation coefficient of 8.4 (-5) cm^{-1} = 2.56 (-3) ft^{-1}. The source is assumed to have an intensity of 0.75 (+15) MeV/shot with an isotropic distribution. Calculated results are listed in Table 6.

3.5.2. Skyshine Method II

This method should give more accurate results since the input data is based on Monte Carlo calculations and the method does not rely on buildup factors or correction factors. In Ref. 10 is published an extensive set of curves relating the air-scattered gamma-ray tissue dose rate to a source photon emission rate at various beam angles and source-detector separation distances, for different photon energies.

The curves show clearly that the scattered dose rate is inversely proportional to separation distance. Hence, all skyshine dose rates can be calculated for 100 ft, and later corrected to other distances.*

For this study, the following steps were performed:

a. Dose rate was plotted against beam angle for a constant separation distance of 100 ft and for source photon energies of 0.6 and 1 MeV, and the results averaged.

b. Dose rate units were changed from

$$\frac{\text{R/hr}}{\text{Source photons/sec}} \text{ to } \frac{\text{mR}}{\text{Source MeV}} .$$

Figure 9 shows the composite plot, which forms the basis for the Method II analysis.

---

*Note that the Method I results did not conform to this relation.

TABLE 6
SKYSHINE DOSES (METHOD I)

Detector Location	Separation Distance (ft)	Horizontal Range (mfp)	K'_s	B_∞	W	G(ω)	S_{sky}(mR/shot)
Control Room	100	0.256	1.35	1.24	1.0	1.0	0.39
					0.826	0.6	0.234
					0.742	0.5	0.196
Guard Shack	240	0.615	1.1	1.65	1.0	1.0	0.102
					0.826	0.6	0.062
					0.742	0.5	0.052
Dunhill Street	280	0.72	1.0	1.79	1.0	1.0	0.076*
					0.826	0.6	0.046*
					0.742	0.5	0.038*

*These would increase if limiter bremsstrahlung were included.

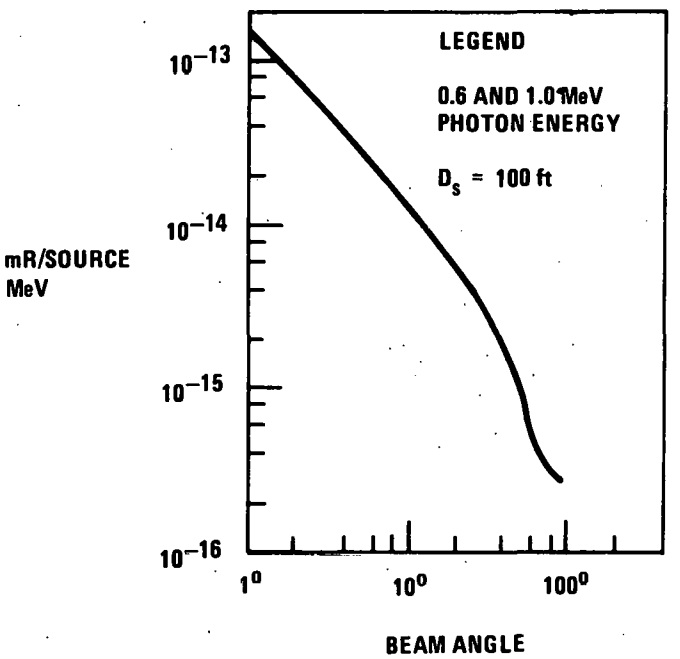

Fig. 9. Photon air scattering functions from "Reactor Handbook-Shielding"

If one simply makes the same source assumption as in Method I -- isotropic point source, solid angle fraction of 1.0, 100 ft separation distance -- Fig. 9 produces the results found in Table 7.

TABLE 7
SKYSHINE DOSE COMPARISON METHOD I VS METHOD II

Angular Increment	Fraction of Spherical Surface	Mean Air Scattering Function from Fig.	Products
0 - 3°	0.00068	8 (-14)	0.54 (-16)
3 - 6°	0.00205	3.2 (-14)	0.66
6 - 10°	0.00486	1.6 (-14)	0.78
10 - 15°	0.0094	9.5 (-15)	0.89
15 - 20°	0.0131	6 (-15)	0.79
20 - 30°	0.0131	3.8 (-15)	1.40
30 - 45°	0.0795	2 (-15)	1.60
45 - 60°	0.1035	9 (-16)	0.93
60 - 90°	0.25	3.5 (-16)	0.88
			8.47 (-16)

Hence, Method II $S_{sky} = \frac{8.47\ (-16) \times 0.75\ (+15)}{2} = 0.32$ mR/shot,

as compared with the Method I result of 0.39 mR/shot; and agreement for this one idealized case is quite satisfactory.

R. D. Seraydarian performed a study to determine the proper correction factors to use with Method II when a solid angle fraction is less than unity. These factors are listed in Table 8.

TABLE 8
G(ω) FACTORS FOR METHOD II

Scattering Angle	90°(1-ω)				
	0°	10°*	15°	17°	19°
0 - 10°	1.0	0	0	0	0
10 - 20°	1.0	0.45	0.1876	0.0884	0.0167
20 - 30°	1.0	0.725	0.5778	0.5090	0.4305
30 - 45°	1.0	0.81	0.7189	0.6792	0.6384
45 - 60°	1.0	0.855	0.7876	0.7587	0.7297
60 - 90°	1.0	0.885	0.8250	0.8017	0.7780

*Estimated.

In the interest of conservatism, it is again assumed that the shield subtends an angle of 10° at the source (Fig. 5). Table 9 shows the calculations for the control room, which is 100 ft from the Inconel bremsstrahlung source.

TABLE 9
METHOD II SKYSHINE CALCULATION FOR CONTROL ROOM

Scattering Angle	Fraction of Spherical Surface	Mean Air-Scattering Function	Preferential Emission Factor	G(ω)	Products
10 - 20°	0.0225	7.5 (-15)	1.4	0.45	1.06 (-16)
20 - 30°	0.368	3.8 (-15)	1.05	0.725	1.07
30 - 45°	0.0795	2 (-15)	0.75	0.81	0.96
45 - 60°	0.1035	9 (-16)	0.5	0.855	0.40
60 - 90°	0.25	3.5 (-16)	0.325	0.885	0.25
					3.74 (-16)

whence S_{sky} (control room) = $\frac{3.74\ (-16) \times 0.75\ (+15)}{2}$ = 0.07 mR/shot

and using the inverse-R relation,

S_{sky} (guard shack) = $\frac{100}{240} \times 0.07$ = 0.029 mR/shot.

As discussed earlier, the calculation of the skyshine dose at Dunhill Street -- or at any detector locations forward of the limiter beam -- should include an estimate of the contribution from this source. The layout is sketched in Fig. 10.

For the reference distance and direction of 280 ft to Dunhill Street, the detector is about 90° off the limiter beam direction, for which the preferential emission factor is 0.38 for tantalum according to Table 3 or 0.33 for Inconel according to Fig. 4. However, the situation is completely non-isotropic, both azimuthally and in polar angle. An estimate will be made in Table 10 for just the 10 - 20° azimuthal segment. The results should be compared with 5.3 (-17) contribution from the Inconel vacuum chamber wall. However, the tantalum limiter bremsstrahlung source strength would be a factor of 2.7 higher. Hence, the tantalum limiter would increase the chamber wall skyshine dose by 30%, while the Inconel limiter would increase it only by 10%.

3.6. TOTAL DOSES

The direct, structure-scattered, and skyshine doses calculated in the preceding sections are summarized in Table 11.

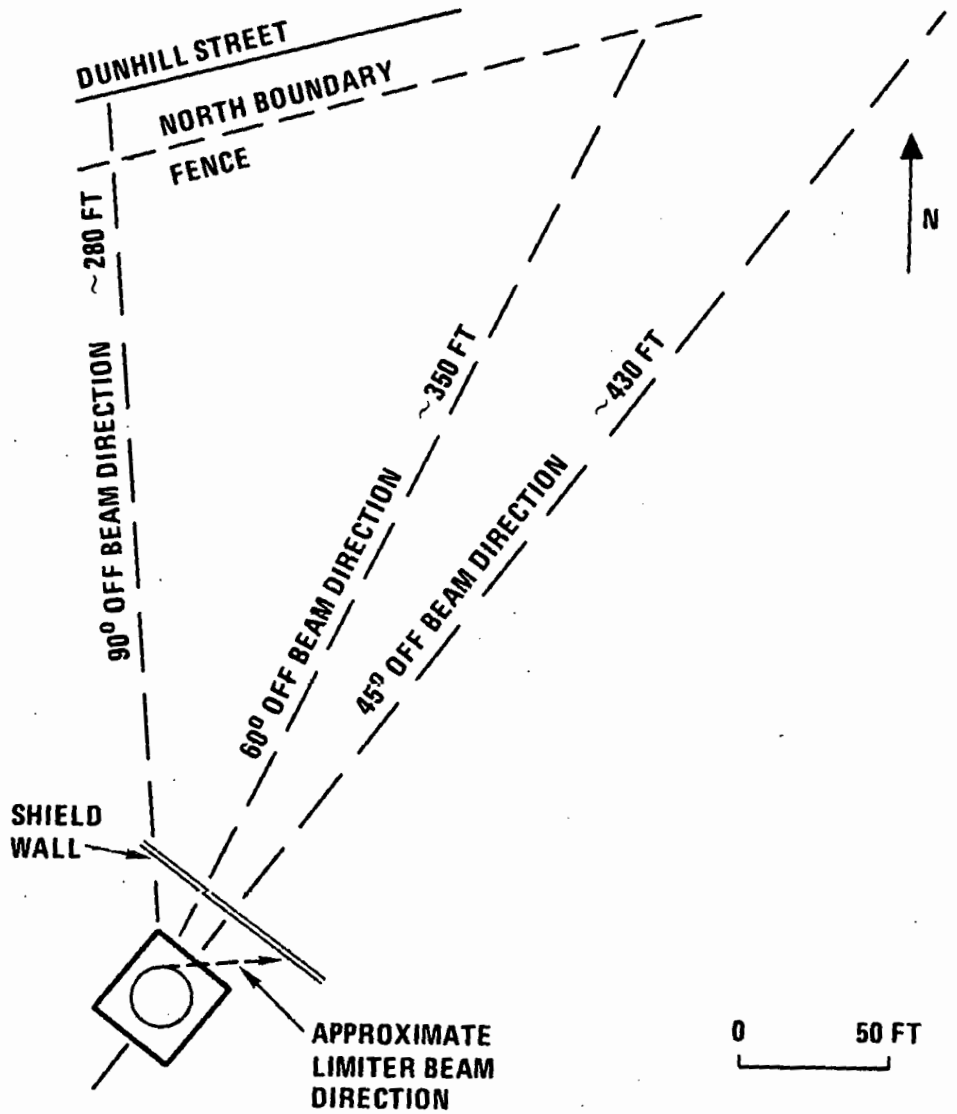

Fig. 10. Layout for north boundary skyshine calculation

TABLE 10
ESTIMATE OF LIMITER CONTRIBUTION

Polar Angular Segment Off Beam Direction	Fraction of Spherical Surface	Mean Air-Scattering Function	Preferential Emission Factor		Products	
			Tantalum	Inconel	Tantalum	Inconel
0 - 10°	0.000625	3.5 (-16)	1.58	2.41	0.35 (-18)	0.53 (-18)
10 - 20°	0.000625		1.31	1.85	0.29	0.41
20 - 30°	0.000625		1.04	1.40	0.23	0.31
30 - 45°	0.00093	9 (-16)	0.82	0.98	0.7	0.8
45 - 60°	0.00093	2 (-15)	0.60	0.63	1.1	1.2
60 - 90°	0.00125	~ 5 (-15)	0.44	0.42	2.7	2.6
					5.4 (-18)	5.8 (-18)

TABLE 11
RUNAWAY SHOT DOSE SUMMARY
(mR/shot)

Location	Direct	Structure Scattered	Skyshine[a]	Total
Control Room	nil	0.34	0.07	0.41
Guard Shack	nil	0.026	0.029	0.045
Dunhill Street	nil	0.02	0.032[b], 0.027[c]	~0.05

[a] Conservatively assuming shield subtends angle of only 10°.
[b] Tantalum limiter.
[c] Inconel limiter.

3.7. COMPARISONS WITH MEASUREMENTS

Numerous gamma dose measurements have been made by J. D. Jones, Safety Engineer, since the startup of Doublet III in early 1978. Most of the measurements represent the integrated dose from numerous shots over several-week periods, as recorded on personnel film badges. Low-range (200 mR) and high-range (5,000 to 20,000 mR) dosimeters are also used; these can be reset after each shot or group of shots.

Figure 11 shows some of the integrated film badge readings recorded by J. D. Jones. These readings encompassed the period Nov. 3, 1978 through Feb. 1, 1979. Three film badges are generally used at each location -- 5, 8, and 11 ft above floor level.

There is no way to tell how many runaway shots are included in these doses. However, it can be seen that the doses off the limiter (3200 mR max) are, indeed, higher than the general level in other directions, by a factor of approximately five. At this time, a tantalum limiter was being used.

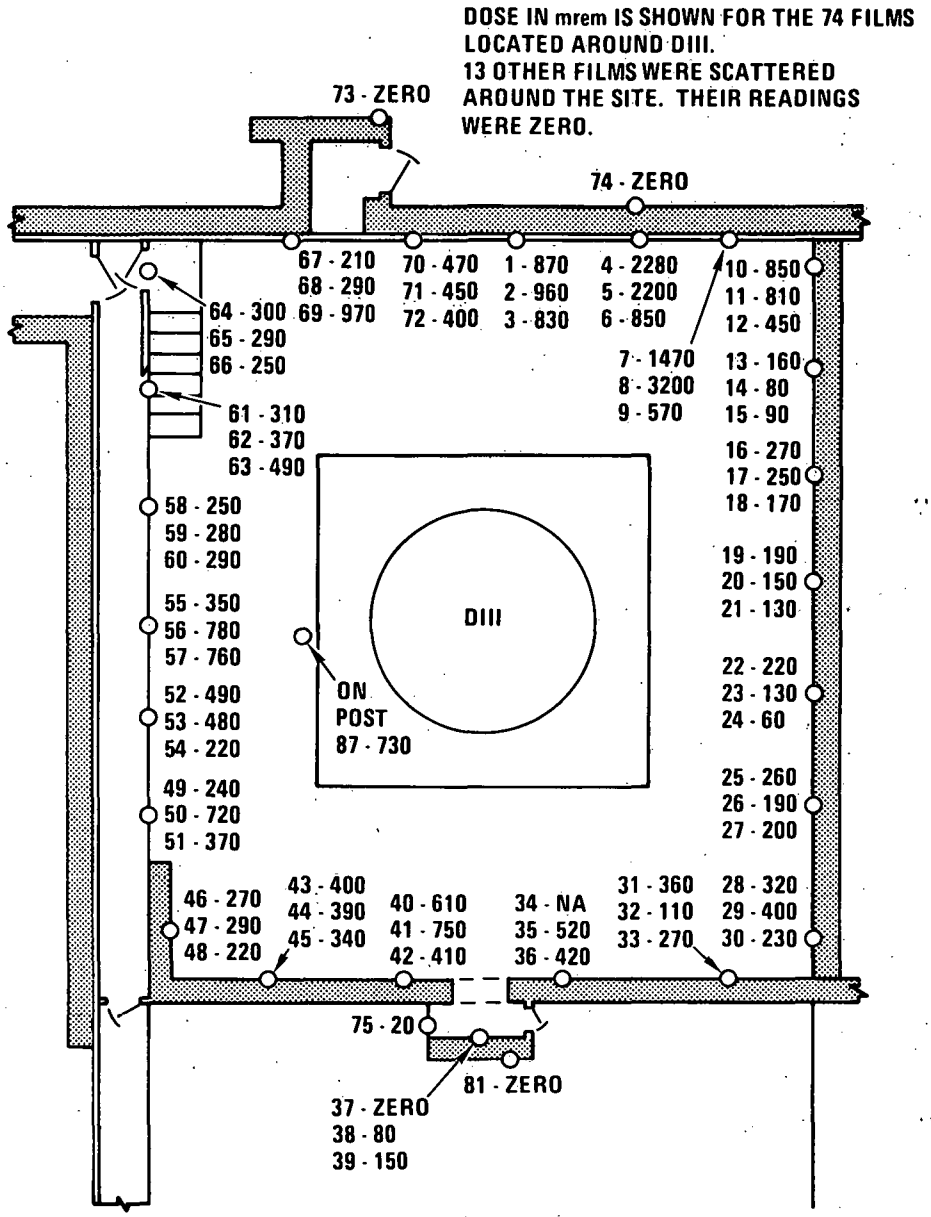

Fig. 11. Film badge radiation readings for operating period 11/3/78 thru 2/1/79

Hence, the prediction in Table 4 -- that the dose at unshielded Detector D would be about three times higher than at unshielded Detectors B or C -- is at least qualitatively borne out. Note that all doses outside the shield walls are zero. If the minimum dose which can be detected is 10 mR, then Table 4 shows clearly why nothing was observed, since the wall attenuation is typically 0.001.

Occasional shots which manifest runaway electrons are recorded separately. Shots 6843 and 6845 on November 27, 1979 characterize the peak runaway current calculated by Hsieh. Individual readings taken on dosimeters by J. D. Jones were averaged for the two shots, and listed in Table 12. Locations of the dosimeters are shown in Fig. 12.

Calculated values shown in the table are generally equal to or lower than measured values. It appears that the calculated direct, unshielded doses agree best with measurements, thus signifying that the source term for the runaway shots is approximately correct.

The underestimate at Point 4 is likely due to the measurement being made on the staging area side of the control room wall, while the calculation was made inside the control room. The disagreement at Point 2 probably arises from scattered radiation from the barrier at the machine pit entry way, not accounted for in the direct dose calculation. It is estimated that 1.5 mR at D_2 could be produced from this source if the concrete albedo is 0.1. The measured dose at D_6 may similarly include some radiation scattered through the north entryway.

It can be concluded that the measured X-ray dose at the control room and the calculated doses at the guard station and north boundary (Dunhill Street) are very low, even for these worst-case runaway electron shots, and hence the shield design shown in Figs. 4 and 12 is entirely adequate for non-beam-line operation of Doublet III.

TABLE 12
COMPARISON OF MEASURED AND CALCULATED X-RAY DOSES
AT DOUBLET III DUE TO RUNAWAY ELECTRON SHOT

Measured Values		Calculated Values				
Detector Number	Dose (mR)	Detector Number	Direct Dose (mR)	Wall and Ceiling Scattered Dose (mR)	Air-Scattered Dose (mR)	Total Dose (mR)
D_1^M	400	D_1^C	440[a]	Unimportant	Unimportant	440
D_2^M	1.5	D_2^C	0.042	0.7 (est.)	0.14	0.9
D_3^M	<1	Not calculated				
D_4^M	1.5	D_4^C (control room)	0.004	0.34	0.07	0.4
D_5^M	140[b]	D_5^C	140[c]	Unimportant	Unimportant	140
D_6^M	2	D_6^C	0.064	0.7 (est.)	0.14	0.9
Undetectable		D_8^C (guard station)	0.004	0.026	0.029	0.06
Undetectable		D_9^C (north boundary)	Nil	0.02	0.03	0.05

[a] Assuming 3.66-m (12 ft) separation from equivalent point source.
[b] Behind 1.3-cm (0.5-in.) steel auxiliary shield.
[c] Without auxiliary shield.

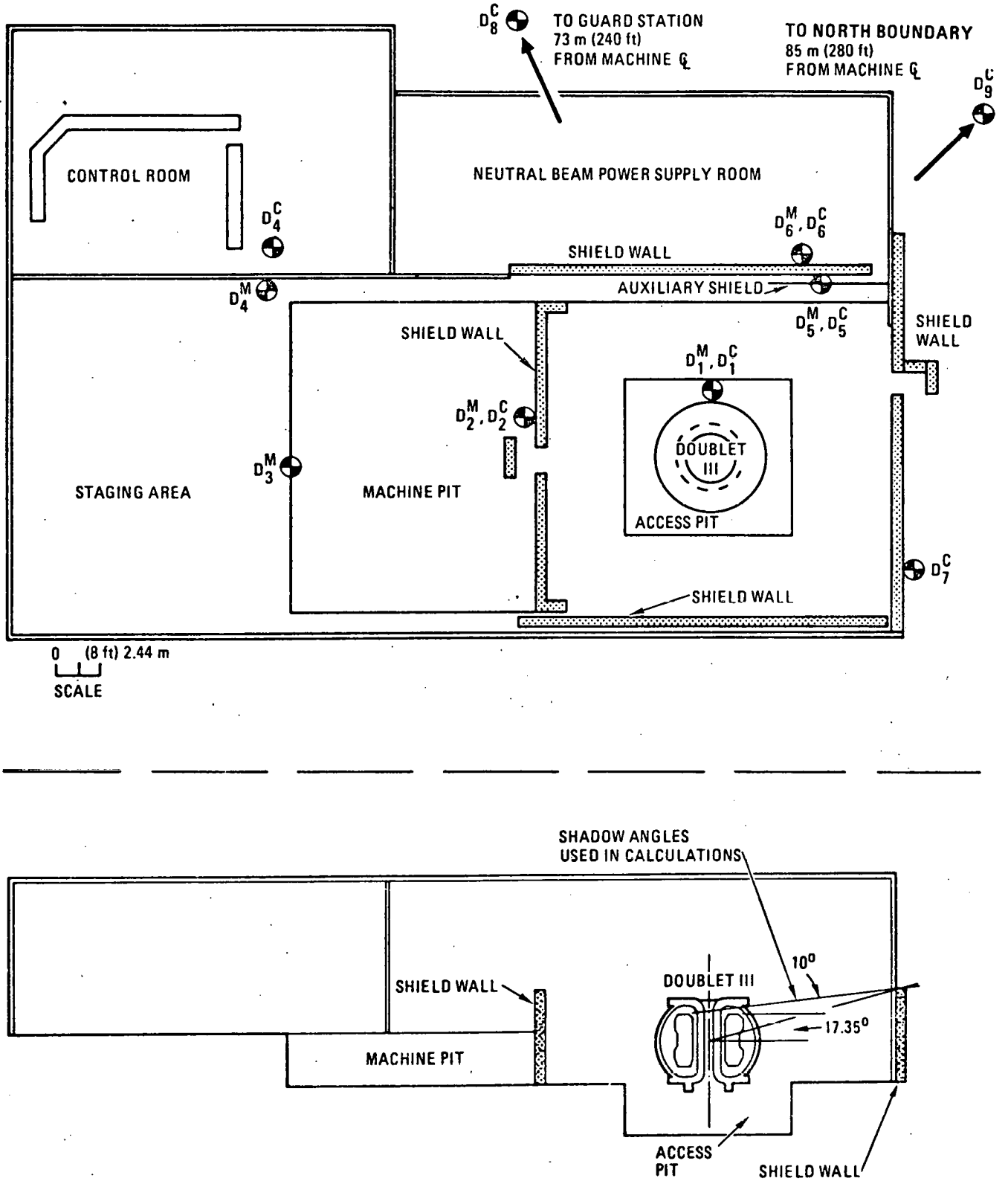

Fig. 12. Configuration for Doublet III shielding calculations

4. NEUTRON SHIELDING ANALYSIS

Operation of Doublet III with neutral beam injection in 1981 and subsequent upgrading in 1981-1983 creates the possibility of D-D and D-T neutron generation at some future time. Shielding analysis and design was performed for Doublet III in order to identify the radiation problems and shielding requirements and costs associated with this operational mode.

4.1. PRELIMINARY CALCULATIONS

4.1.1. Source Terms

Reference 11 discusses the implications of neutron production in Doublet III and provides the source terms of Table 13.

The source terms in Table 13 can be compared with those projected for PDX, namely, 10^{15} D-D neutrons per sec and 5×10^{12} D-T neutrons per sec (Ref. 2). These figures are about one-third of Doublet III Phase II operation, i.e., a fusion power of about 1.0 kW.

The dose conversion factors are found from ANSI Standard ANS 6.1.1-1977 to be:

2.5 MeV	1.25(-04) rem/hr // n/cm^2-sec
14 MeV	2.08(-04)

In terms of integrated exposure and mrem instead of rem, the conversion factors are:

2.5 MeV	3.47(-05) mrem//n/cm^2
14 MeV	5.78(-05)

TABLE 13
POSSIBLE D-III NEUTRON PRODUCTION[11]

	Phase I	Phase II	Phase III-a	Phase III-b	Phase III-c
Peak Temperature (keV)	0.7	2.8	4.8	7.2	7.4
Peak Density (cm^{-3})	6×10^{14}	4×10^{14}	4×10^{14}	4×10^{14}	4×10^{14}
Beam Power (MW)	0	7	14	21	21
$D + D \rightarrow {}^{3}He + n$ (sec^{-1})	4×10^{12}	3×10^{15}	2×10^{16}	6×10^{16}	7×10^{16}
$D + D \rightarrow T + p$ (sec^{-1})	4×10^{12}	3×10^{15}	2×10^{16}	6×10^{16}	7×10^{16}
$D + T \rightarrow {}^{4}He + n$ (sec^{-1})	3×10^{9}	1.3×10^{13}	2×10^{14}	9×10^{14}	1.0×10^{15}
Fusion Power (kW)	4.7×10^{-3}	3.0	22	75	82

4.1.2. Dose Criteria

The most important dose criterion for a study of the Doublet III upgrade is the permissible annual dose at the site boundary, i.e., on Dunhill Street (see Fig. 10). Nuclear power stations are now limited by NRC interpretation of 10CFR50 to 5 mrem/year per unit at the site boundary. For purposes of this study and considering that a shorter-lived single device is involved, it was agreed with GA Health Physics that 25 mrem would be acceptable for the annual site boundary exposure. The shielding calculations can easily be scaled to any other dose criterion, if desired.

The following radiation limits were used in the subsequent shielding calculations:

Radiation worker annual exposure	1,000 mrem/yr
Radiation worker hourly dose rate assuming 40-hr week, 50 wks/yr	0.5 mrem/hr
Site boundary annual dose	25 mrem
Site boundary dose rate	0.003 mrem/hr

4.1.3. Direct Shielding

Existing shielding by the machine itself was assumed in earlier studies by T. J. Woods to consist of 0.5 cm steel plus 10 cm copper. Reference 12 gives the fast neutron attenuation length when not followed by a hydrogenous medium as 16 cm, corresponding to a cross section of 0.72 barns; but if followed by a hydrogenous medium (i.e., water or concrete) iron has a removal cross section of 1.98 b and copper a cross section of 2.04b (Ref. 13). In the case of 14 MeV neutrons, copper has an (n, 2n) cross section of about 0.6 to 0.7b, so one can consider the attenuation of 2.45 and 14 MeV neutrons somewhat similar in copper. Therefore, for direct shielding hand calculations, initial attenuation in the machine is about

$$\exp\left(-\frac{0.6 \times 2.04 \times 9 \times 10.5}{64}\right) = 0.16$$

and for unshielded direct and scattered calculations is

$$\exp\left(-\frac{10.5}{16}\right) = 0.52 \quad .$$

Moving on to concrete, the fission-neutron removal cross section for ordinary concrete is 0.086 cm^{-1} (Ref. 14), whereas the total cross sections are 0.14 cm^{-1} for 2.45 MeV neutrons and 0.12 cm^{-1} for 14 MeV neutrons[15]. On the other hand, Ref. 16 gives values of Σ_R = 0.14 cm^{-1} for 2.45 MeV neutrons and Σ_R = 0.07 cm^{-1} for 14 MeV neutrons (See Fig. 13) For purposes of the brief preliminary calculations, an overall removal cross section of 0.1 cm^{-1} was used for both neutron energy groups in ordinary concrete.

With respect to heavy concrete, Ref. 17 gives the total cross section of ferrophosphorous concrete (density = 4.57 g/cc) as 0.22 cm^{-1} for 2.45 MeV neutrons and 0.165 cm^{-1} for 14 MeV neutrons. It is not believed that the improvement in the 14 MeV total cross section from 0.12 cm^{-1} to 0.165 cm^{-1} is worth the expense of going to heavy concrete (the ordinary-to-heavy thickness ratio would be 1:0.73, but the weight ratio would be 1:1.4).

Scattering off the concrete floor surrounding the machine (concrete albedo ≃ 0.6) is likely to increase the dose rate by one-third.

For a detector point 40 ft from the source, shielded by two feet of concrete, we have for Phase II

$$\text{dose} = \frac{1.33 \times 0.16}{4\pi(40 \times 30.5)^2} \times e^{-0.1 \times 61} \left[3(+15) \times 3.47(-05) + 1.3(+13) \times 5.78(-05)\right]$$

= 2.8 mrem per shot.

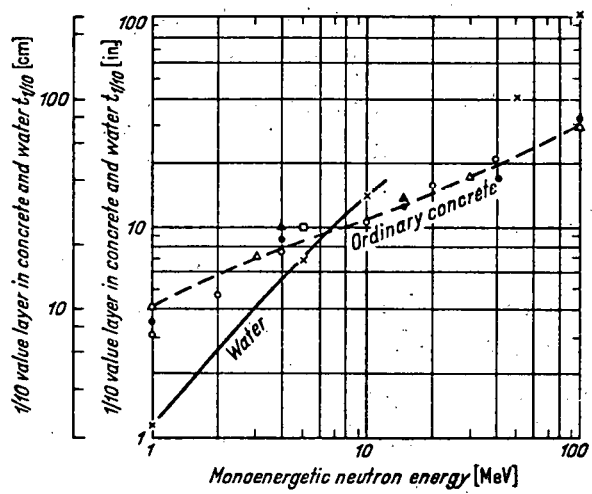

Fig. 13. Tenth-value layers in concrete and water, as a function of monoenergetic neutron energy (from Ref. 16)

Other points are calculated and plotted in Fig. 14 and some specific direct doses with the existing shielding are shown in Fig. 15.

From the standpoint of direct doses, to achieve 0.5 mrem/shot in the control room (necessary for a schedule of one shot per hour), the existing shielding is adequate for Phase II but would have to be increased to 3 ft for Phase III-b operation.

Presumably, access control would be exercised in the machine pit, neutral beam power supply room, B coil power supply room, and other areas immediately adjacent to the Doublet III room. If not, Fig. 15 shows that the dose of 2.8 mrem would have to be reduced to 0.5 mrem, requiring an additional half foot of ordinary concrete. Additional concrete shielding would also be needed in the direction of Dunhill Street.

4.1.4. Shield Penetrations

Some of the shield penetrations shown in Fig. 12 are inadequate in a fast-neutron environment. For example, the accessway to the machine pit would have to be modified as illustrated in Fig. 16.

If the Doublet III room is eventually to be completely enclosed by concrete walls, there will exist a higher neutron population owing to the high concrete albedo. Total flux levels in the area might be a factor of two higher than the unscattered flux. Furthermore, the scattered component will have random directions. Hence, piping and electrical penetrations through the concrete shield walls cannot be designed assuming a radially directed flux from the Doublet III centerline.

4.1.5. Wall Scattering

With the Doublet III room completely enclosed by concrete walls and roof, wall scattering would be of little or no consequence to personnel occupying the control room. For illustrative purposes, however, a rough

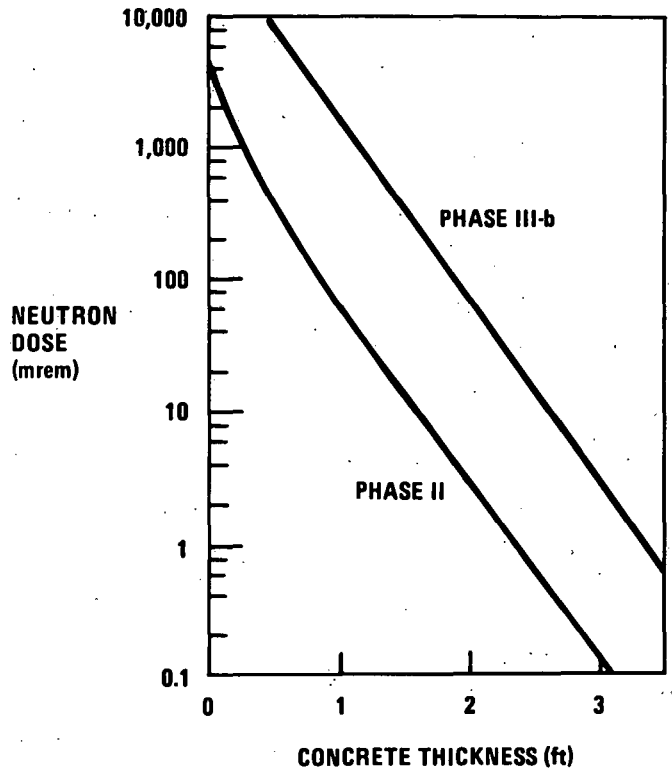

Fig. 14. Direct neutron dose as a function of ordinary concrete thickness; single pulse, 40-ft separation distance

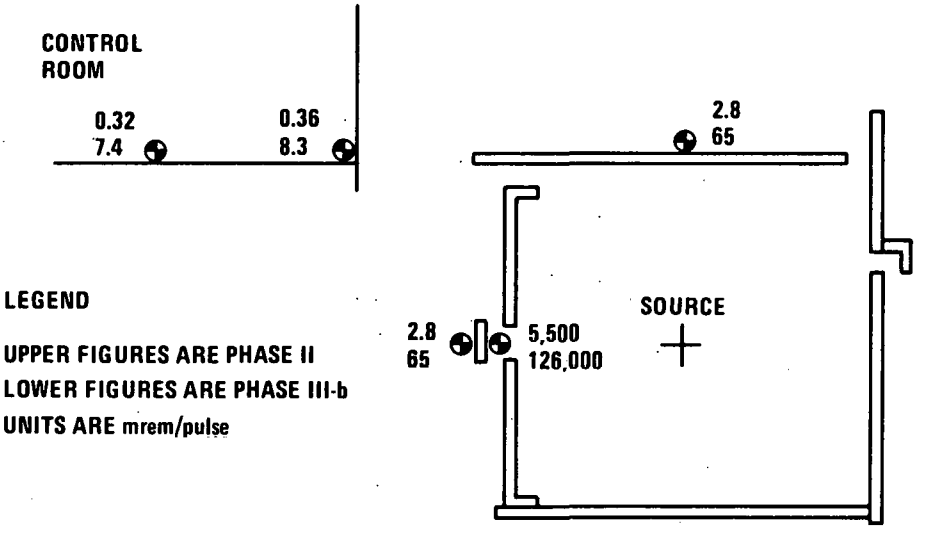

Fig. 15. Direct neutron doses from single pulse with existing ordinary concrete shielding

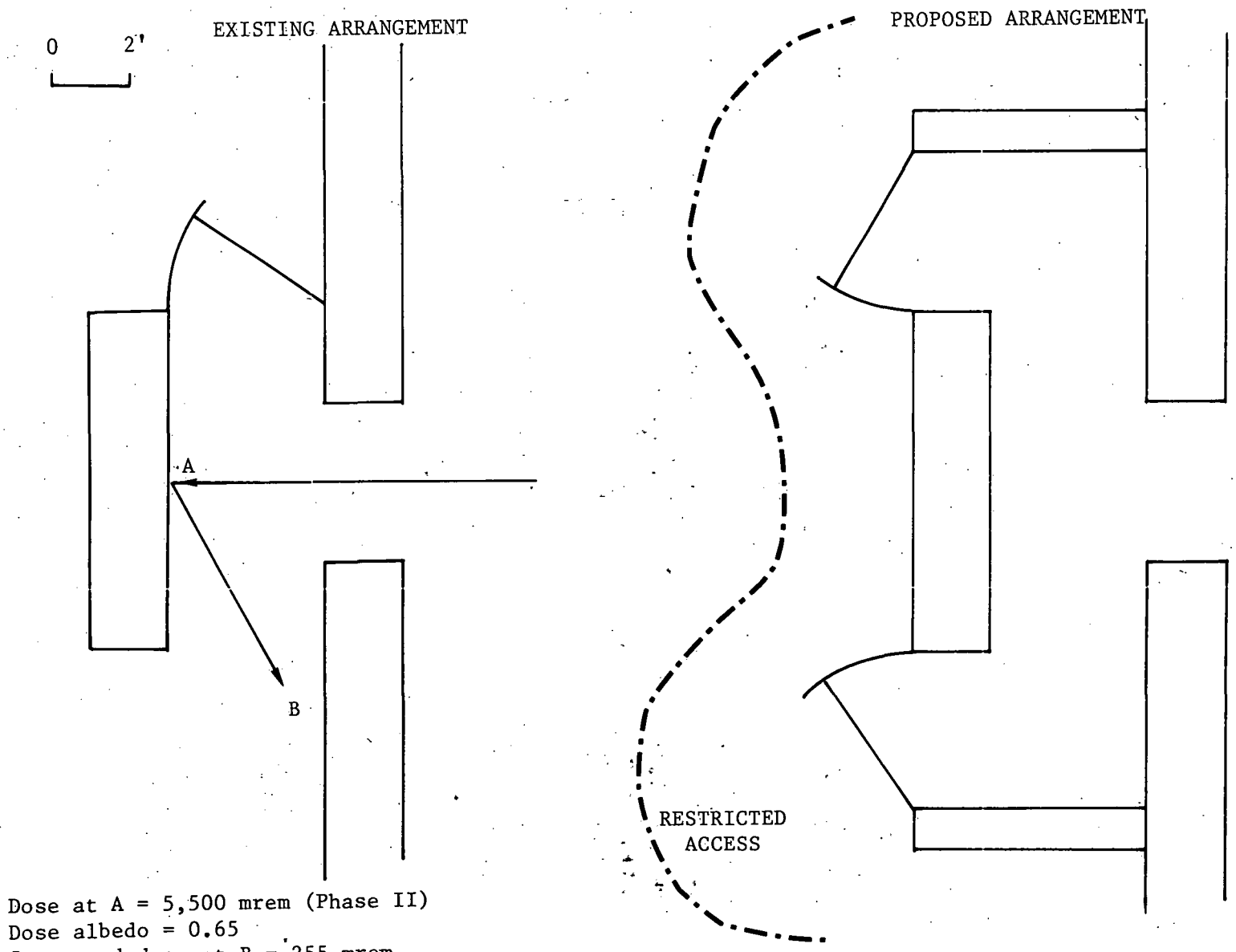

Fig. 16. Proposed entryway modification

hand calculation was performed for the unshielded geometry shown in Fig. 7. Only the scattering from wall No. 1 was considered. The resulting dose in the center of the control room is 20 mrem per pulse (Phase II); inclusion of wall No. 2 and the ceiling might increase this dose to 50 mrem. Since this dose is considerably higher than the direct dose of 0.3 mrem, it is obvious that wall and ceiling scattering cannot be tolerated.

4.1.6. Air Scattering

Air scattering (skyshine) is expected to be the predominant contributor to the site boundary dose, and control thereof will dictate the required upper wall and roof shielding thicknesses.

Air-scattered fast-neutron dose rates are plotted in Ref. 18 for several discrete neutron energies. The only difference between the plots for 2.7 MeV and 14 MeV appears to be the dose conversion factor; hence, all the neutrons will be assumed to have 2.7 MeV energy. A plot of the scattered neutron fluence vs. beam angle for 100 ft separation and a single source neutron is shown in Fig. 17.

Using the approach of Section 3.1.3., it is now necessary to calculate the fraction of source neutrons that are emitted at various beam angles, taking account of shadowing by existing shield walls and floor. By superimposing spherical surfaces divided off into shadow angles, one can estimate the fraction of each angular band which can "see" above the shield wall.

Table 14 shows the calculation of the air-scattered neutron fluence 100 ft from Doublet III in the direction of Dunhill Street. The total is 1.29(-9) n/cm^2 per source neutron. Since the air-scattered dose is generally inversely proportional to distance, the Dunhill Street fluence would be $\frac{100'}{280'}$ x 1.29(-9) = 4.6(-10) n/cm^2-n. Multiplying by the source strength and converting to mrem yields the following unshielded air-

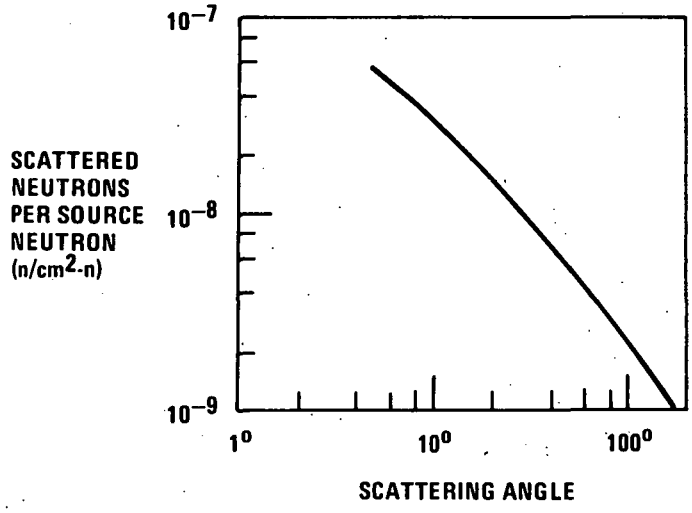

Fig. 17. Neutron scattering function

Table 14

AIR-SCATTERED NEUTRON CALCULATIONS

ANGULAR INTERVAL	FRACTION OF SURFACE $\left(\frac{\cos\theta_1 - \cos\theta_2}{2}\right)$	FRACTION CORRECTED FOR NORTH WALL	SCATTERING FNC(cm^{-2})	PRODUCT
10^o-20^o	0.022	0.0032	2.0-8	0.64-10
20^o-30^o	0.037	0.0107	1.1-8	1.8-10
30^o-40^o	0.05	0.0175	7.8-9	1.37-10
40^o-50^o	0.062	0.0236	5.8-9	1.37-10
50^o-60^o	0.072	0.0281	4.6-9	1.29-10
60^o-70^o	0.079	0.0316	3.7-9	1.17-10
70^o-80^o	0.084	0.0344	3.0-9	1.03-10
80^o-90^o	0.087	0.0365	2.6-9	1.95-10
90^o-100^o	0.087	0.0365	2.3-9	0.84-10
100^o-110^o	0.084	0.0344	2.0-9	0.69-10
110^o-120^o	0.079	0.0316	1.8-9	0.57-10
120^o-130^o	0.072	0.0281	1.6-9	0.45-10
130^o-140^o	0.062	0.0236	1.45-9	0.34-10
140^o-150^o	0.050	0.0175	1.3-9	0.23-10
150^o-160^o	0.037	0.0107	1.2-9	0.13-10
160^o-170^o	0.022	0.0032	1.1-9	0.04-10
				1.23-9 cm^{-2}

scattered doses at Dunhill Street per pulse:

Phase II	33 mrem
Phase III-b	760 mrem
(Annual Limit	25 mrem)

The amount of ordinary concrete shielding needed to attenuate these air-scattered doses to acceptable levels is tabulated in Table 15. Fig. 14 was used to arrive at these estimates.

Some of these air-scattering results are also shown in Fig. 18.

4.1.7. Total Doses

Table 16 summarizes the preliminary shielding recommendations.

Better calculations would be needed to provide assurance of the correct shielding thicknesses for the site boundary dose. In particular, the preliminary calculations did not treat the angle of incidence rigorously, and did not allow for a possible difference between wall thickness and roof thickness (it is preferable to minimize the roof thickness). Also, the increasing importance of 14 MeV neutrons and capture gammas with increasing concrete thickness was not taken into account. The subsequent sections describe more sophisticated follow-on calculations.

4.2. COMPARISONS WITH LITERATURE

Comparisons were made between DIII skyshine and direct dose levels and those from other studies in order to assure the adequacy of the preliminary shield thicknesses.

Table 17 lists some of the skyshine information extracted from the literature and aptly demonstrates the wide divergence of results in the area of skyshine analysis and shield design. Taking the 14 MeV neutron

Table 15

EFFECT OF ORDINARY CONCRETE SHIELDING
ON DUNHILL STREET AIR-SCATTERED NEUTRON DOSE

		Phase II		Phase III-b	
Assumed angle of neutron incidence on shield		90^{o}	45^{o}	90^{o}	45^{o}
Concrete Thickness	Quantity				
1 ft	mrem/pulse	0.45	0.13	10.5	3
	permissible pulse rate	∿1 per wk	∿4 per wk	∿2 per yr	∿8 per yr
2 ft	mrem/pulse	0.022	0.0018	0.5	0.04
	permissible pulse rate	∿3 per da	∿40 per da	∿1 per wk	∿2 per da
3 ft	mrem/pulse	---	---	0.032	---
	permissible pulse rate	---	---	∿2 per da	---

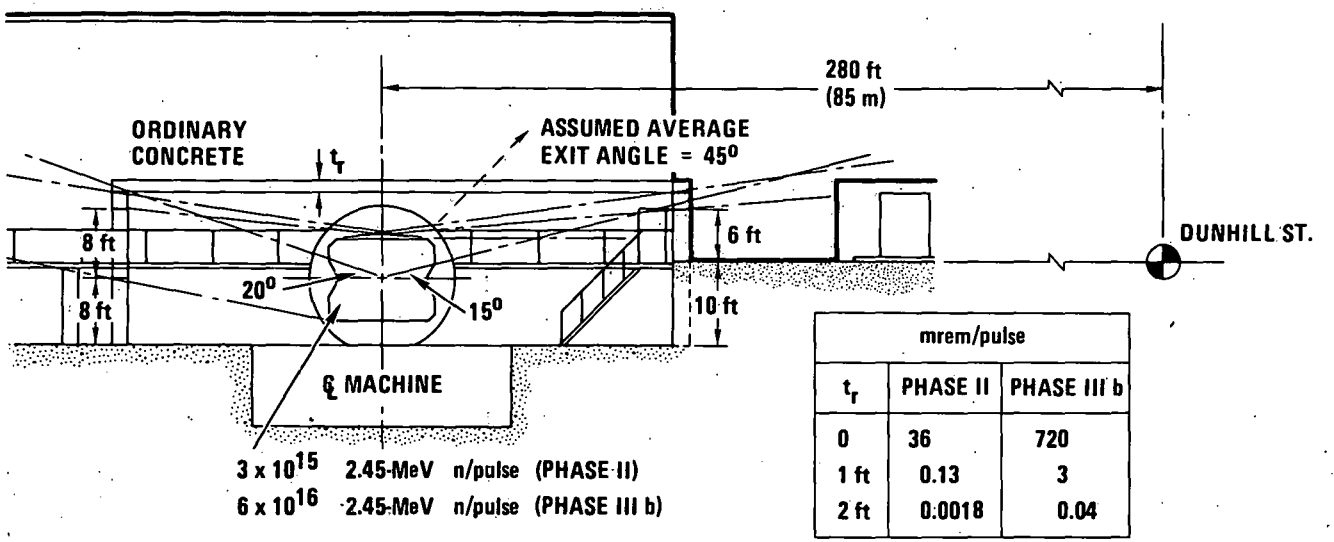

mrem/pulse		
t_T	PHASE II	PHASE III b
0	36	720
1 ft	0.13	3
2 ft	0.0018	0.04

Fig. 18. Doublet III Upgrade neutron shielding

Table 16

SUMMARY OF PRELIMINARY RESULTS

ORDINARY CONCRETE SHIELD REQUIREMENTS

	Phase II		Phase III-b	
	1 shot/da*	24 shots/da	1 shot/da*	24 shots/da
Control Room				
Direct shielding required	**	**	2.25 ft	3 ft
Air scattered shielding required	(Determined by Dunhill Street Dose)			
Dunhill Street				
Direct shielding required***	**	3.2 ft	2.8 ft	3.7 ft
Air scattered shielding required	∿1.5 ft	∿2.5	∿2.5	∿3.5

* During working hours
** Existing shielding is adequate
*** Air attenuation neglected

TABLE 17. SKYSHINE DATA COMPARISON

MACHINE	DOUBLET III		PDX	TFTR	INS	JET		HEGLF
Reference	This Report		2	19	20	21		22
Neutron Source, n/y 14 MeV 2.45 MeV	1.3(+17) 3(+19)		5(+15) 1(+18)	3.6(+21) 0	3.2(+22) 0	5(+23) 0		9(+19) 0
Roof Shield Thickness and Material	0.92 m ordinary concrete		0.38 m borated water	2 m ordinary concrete	2.13 m ordinary concrete	2.5 m ordinary concrete	2.1 m	1.52 m LASL concrete**
Separation Distance	85 m		150 m	125 m	150 m	200 m		42 m
Annual Skyshine Dose, mrem/y	14 (90^{o} incid.)	0.34 (45^{o} incid.)	9	5*	1.8	0.1	3.3	21
Hardware Accounted For?	Yes		No	No	No	Yes		No
Dose Normalized to 100 m Using Fig. 1	11.2	0.27	18	6.7	3.6	0.3	9.9	7
Dose per 14 MeV Neutron, mrem/n-y	---	---	---	1.86(-21)	1.12(-22)	6(-25)	2(-23)	7.8(-20)
Dose per 14 MeV Neutron Normalized to 2 m Ordinary Concrete, Using 0.113 m e-folding Distance, mrem/n-y	---	---	---	1.86(-21)	3.5(-22)	5(-23)	5(-23)	1.1(-21)
Dose per 2.45 MeV Neutron, mrem/n-y	3.7(-19)	9(-21)	1.8(-17)					
Dose per 2.45 MeV Neutron Normalized to 0.61 m Ordinary Concrete Using Data Refs. 1 & 2, mrem/n-y	2(-17)	4.8(-19)	9.7(-17)					

*Assumes total dose of 10 mrem/y of which half is air-scattered and half is direct.
** Density 2.25 g/cm^3

emitters first, one observes a factor of 37 variation in normalized mrem/n-y, from 5(-23) up to 1.86(-21). However, the JET shielding calculation takes into account the TF and PF coils atop the machine; hence, the JET mrem/n-y may be as high as 5(-22) if the hardware were ignored. Therefore, the spread between 14 MeV doses may be more like a factor of 6.

There is a large difference between PDX and DIII results (for the 45^{o} incidence case); the discrepancy is a factor of 200 for 45^{o} incidence. The 90^{o} incidence case is much better, and allowing for the DIII hardware effect, good agreement is attained. However, totally normal incidence is unrealistic.

Further study of PDX results indicates that an important difference is the e-folding distance used. EG&G's ANISN dose calculations, exemplified by Fig. 19, show an initial e-folding length of 0.28 m for 2.5 MeV neutrons, dropping to 0.0555 m at a thickness of 0.6 m. For the DIII preliminary estimates, a constant e-folding distance of 1.10 m was employed. The difference in e-folding values results in a factor of 4 dose difference at 0.6 m thickness.

The PDX results may be somewhat conservative for ordinary concrete, showing a rem e-folding distance in 04 concrete of 0.12 m for 2.45 MeV neutrons, whereas a value of 0.10 m was used in Section 4.1.3. In a 0.61 m shield, this difference would account account for a factor of 2.8 discrepancy in dose.

Further comparisons were made for direct doses, using some of the information available from the previously referenced reports. These comparisons are shown in Table 18.

Again, rather wide discrepancies are noted. The 14 MeV emitters show a range of 4.3(-18) to 3.1(-17), a factor of 7. However, if the JET hardware is ignored, the discrepancy gets worse.

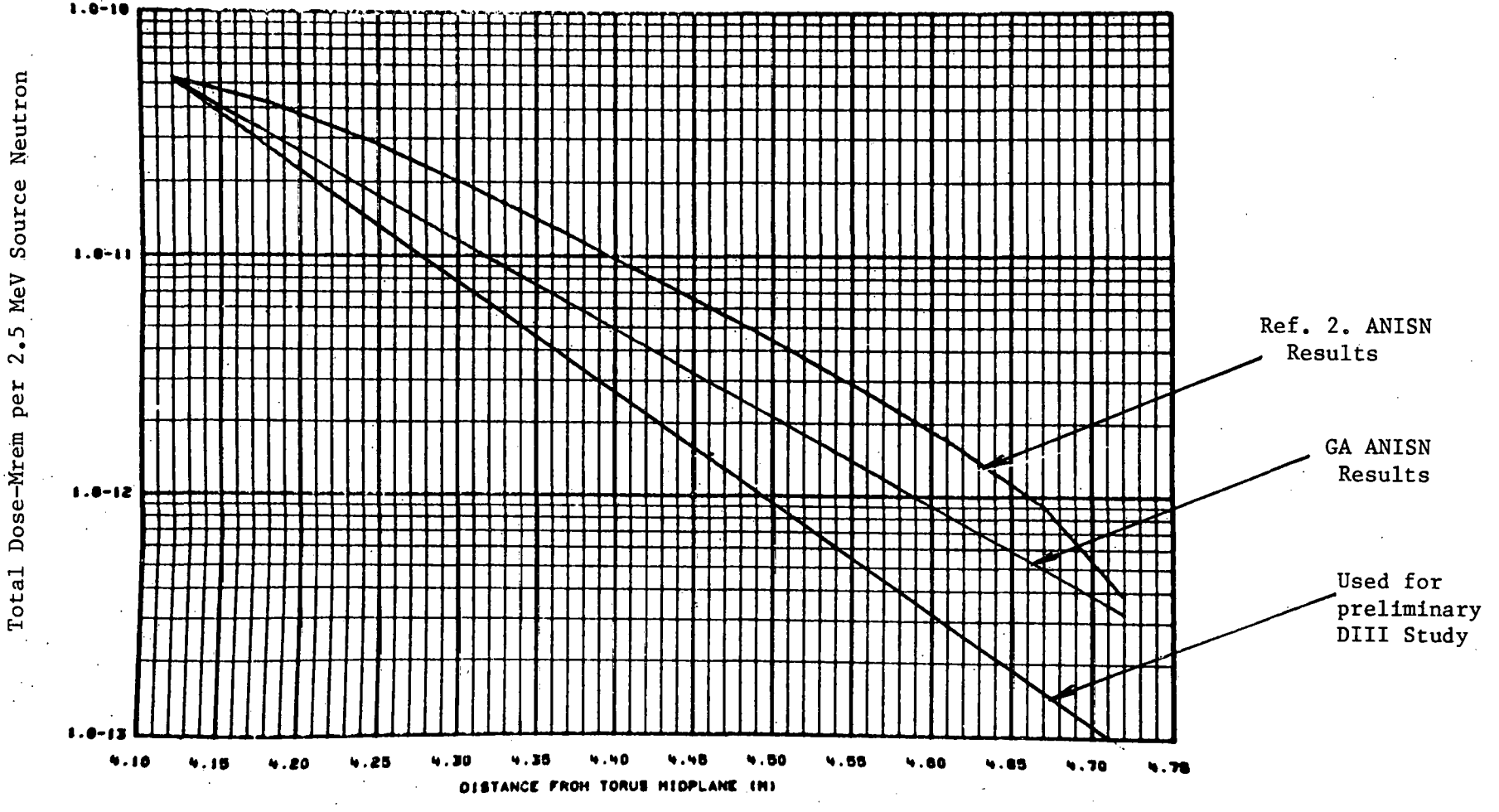

Fig. 19. 2.5 MeV Total Dose Through Type 04 Concrete

TABLE 18. DIRECT DOSE COMPARISON

MACHINE	DOUBLET III	PDX	TFTR	INS	JET	HEGLF
Wall Shield Thickness and Material	1.22 m ordinary concrete	0.81 m heavy concrete	2.19 m ordinary concrete (some boronation)	3.36 m ordinary concrete	3 m ordinary concrete	1.83 m ordinary concrete
Separation Distance	12 m	7.5 m	17 m	NA*	19.5 m	42 m
Annual Direct Dose, mrem/y	53	3,372	1,000	NA	50	140
Dose Normalized to 10 m	91	1,900	2,890	NA	190	2,470
Dose per 14 MeV Neutron mrem/n-y	---	---	8(-19)	NA	3.8(-22)	2.74(-17)
Dose per 14 MeV Neutron Normalized to 2 m Ordinary Concrete, Using 0.113 m e-folding Distance, mrem/n-y	---	---	4.3(-18)	NA	3.1(-17)	6.1(-18)
Dose per 2.45 MeV Neutron, mrem/n-y	3(-18)	3.37(-15)	*Not Available			
Dose per 2.45 MeV Neutron Normalized to 0.92 m Ordinary Concrete Using Data in Refs. 1 & 2, mrem/n-y	6(-17)	2.2(-15)				

The PDX dose again comes out much larger than DIII, by a factor or 30. If the DIII hardware is ignored, the factor is 5. Here again, it seems that PDX is being conservative on the attenuation of 2.45 MeV neutrons through concrete.

The PDX results in Ref. 2 clearly show that the use of heavy concrete is not economically worthwhile. A thickness of 0.53 m heavy concrete is equivalent to 0.60 m of ordinary concrete in dose attenuation, but weighs 40% more.

4.3. DISCRETE ORDINATES CALCULATIONS

An accurate skyshine calculation could be accomplished by several methods: 1) Monte Carlo from source to receptor, 2) discrete ordinates through roof, then Monte Carlo to receptor, 3) discrete ordinates from source to receptor, or 4) some special skyshine routine available from RSIC. Because the two-dimensional discrete ordinates code DOT II was already available and running on the CRAY computer at Livermore, it was decided to set up a single problem describing both the direct and air-scattered fluxes from Doublet III. This problem utilized R-Z geometry, with the vertical axis coinciding with the machine axis, as shown in Fig. 20. An earlier layout had 126 radial intervals and 87 axial intervals, which proved to be excessive for the CRAY storage facilities; the revised version is 71 by 57.

As shown in the figure, the shield roof was assumed to be ordinary concrete except for the region directly over the machine, which consisted of a plastic dome, represented in the transport calculation by polyethelene. Compositions of the relevant materials are listed in Table 19.

The calculations were performed by E. T. Cheng and J. Hildebrand, Jr., using a standard 25-neutron, 21-gamma cross section set.

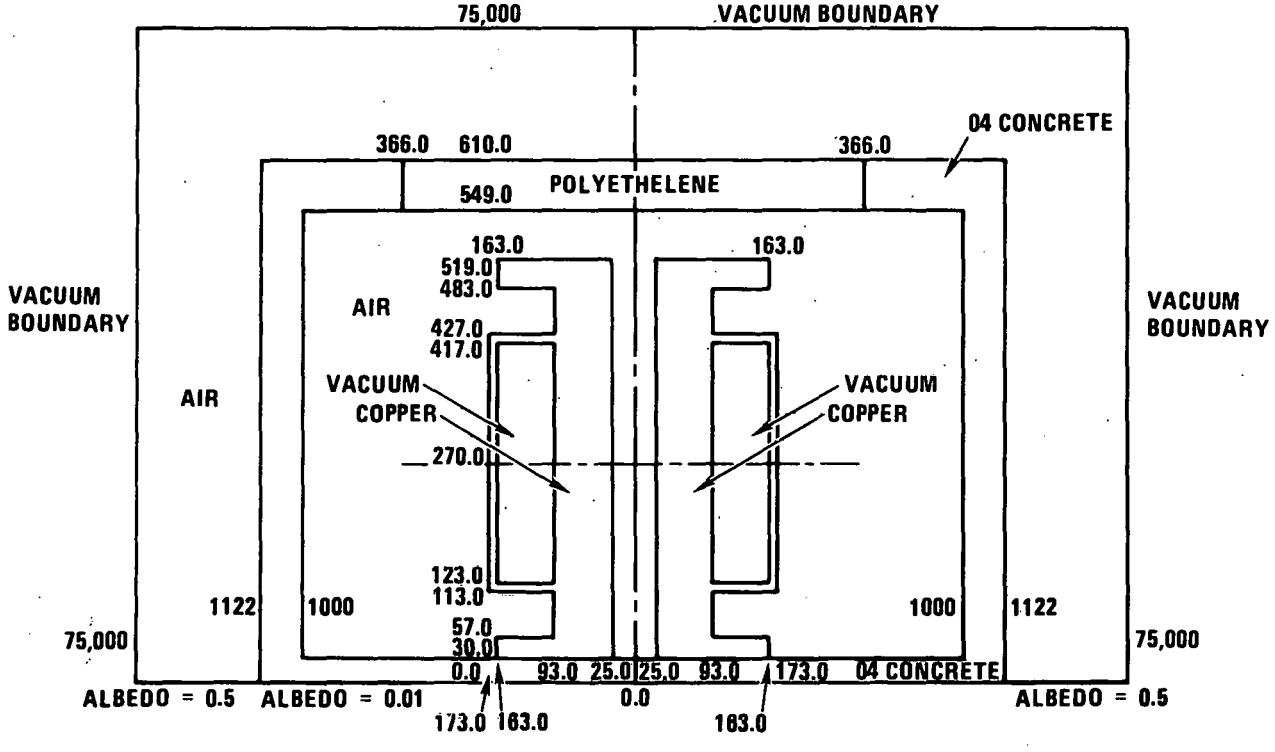

Fig. 20. Model for DOT calculation

Table 19

COMPOSITIONS FOR TRANSPORT CALCULATIONS

Polyethelene	Atoms/barn-cm
H	7.70(-2)
C	3.85(-2)
04 Concrete	
Na	1.048(-3)
Ca	2.916(-3)
Fe	3.128(-4)
Mg	1.486(-4)
O	4.387(-2)
Si	1.581(-2)
H	7.770(-3)
Al	2.453(-3)
K	6.934(-4)
Air	
N	4.20(-5)
O	1.13(-5)
H	8.1(-7)
Soil	
Albedo	= 0.5

The plasma chamber volume was taken as 16.625 m^3; hence, for the Phase II scenario, the neutron source strength and spectrum can be scaled from Ref. 2 and then converted to GA's 46 group cross section set as follows:

Table 20

PHASE II NEUTRON SOURCE TERMS

EG&G Energy Groups

Neutron Energy (MeV)	Volumetric Source Strength (n/m^3 - pulse)
14.92 - 17.33	1.03(+10)
14.19 - 14.92	2.87(+11)
13.50 - 14.19	4.37(+11)
10. - 13.50	4.75(+10)
2.725 - 3.679	6.56(+11)
2.365 - 2.725	1.459(+14)
2.307 - 2.365	2.149(+13)
2.231 - 2.307	1.035(+13)
1.653 - 2.231	2.10(+12)

GA Energy Groups

Group No.	Neutron Energy (MeV)	Volumetric Source Strength (n/m^3 - pulse)
1	13.50 - 17.33	7.34(+11)
2	10. - 13.50	4.75(+10)
13	3.0119- 3.6788	4.58(+11)
14	2.466 - 3.0119	1.05(+14)
15	1.3534- 2.466	7.48(+13)

Flux-to-dose conversion factors were also obtained from Ref. 2 and incorporated into DOT to get biological dose rates.

The DOT II problem was run in both P_1S_4 and P_3S_4 modes for cross comparison. The results were disappointing; the dose rates calculated by DOT were much larger than predicted by other methods or by comparisons with the literature.

The rather large interval size and loose convergence used in the DOT problem were suspect. Therefore, several ANISN runs were set up in spherical geometry as depicted in Fig. 21. The aim was to separate out the effects of different parameter changes such as interval size and angular quadrature. The cases considered are listed in Table 21.

Table 21

PARAMETER SURVEY USING ANISN

Case No.	No. of Mesh Intervals	Angular Quadrature	Convergence
1	71	P_3S_4	10^{-2}
2	71	P_3S_4	10^{-4}
3	126	P_3S_4	10^{-4}
4	126	P_3S_4	10^{-4}
5	152	P_3S_{16}	10^{-4}

Figure 22 shows a summary of the resulting relative doses, including those for DOT (along the doublet midplane). Use of too few mesh intervals does, indeed, result in a higher external dose, as can be seen by comparing ANISN 1/2 with ANISN 3/4 at a radial distance of 1200 cm. However, the DOT dose is still another factor of 7 higher than ANISN 1/2, both of which used about the same mesh spacing in the radial direction.

Agreement between DOT and ANISN is fairly good near the source, as shown in Fig. 23. The ANISN 5 case also agrees fairly well with the EG&G calculation shown in Fig. 19. Just outside the shield, 65% of the dose is due to capture gammas; these could be suppressed by the addition of boron frits such as manufactured by Chi-Vit Corp.

John Hildebrand, Jr. ran several computer plots of neutron and gamma spectra as calculated by ANISN; these are shown in Figs. 24-31. The distances correspond to the ANISN geometry shown in Fig. 21.

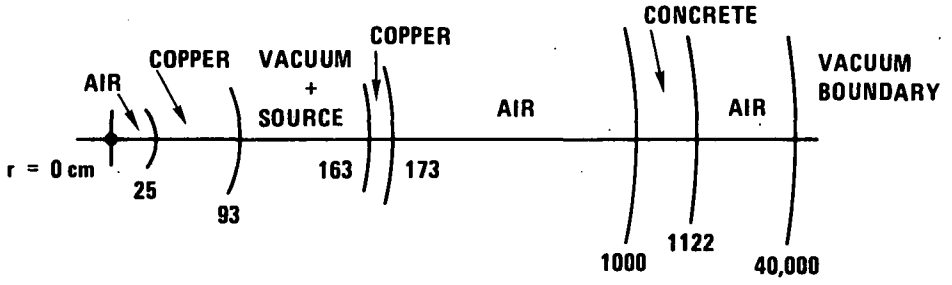

Fig. 21. Model for ANISN calculations spherical geometry.

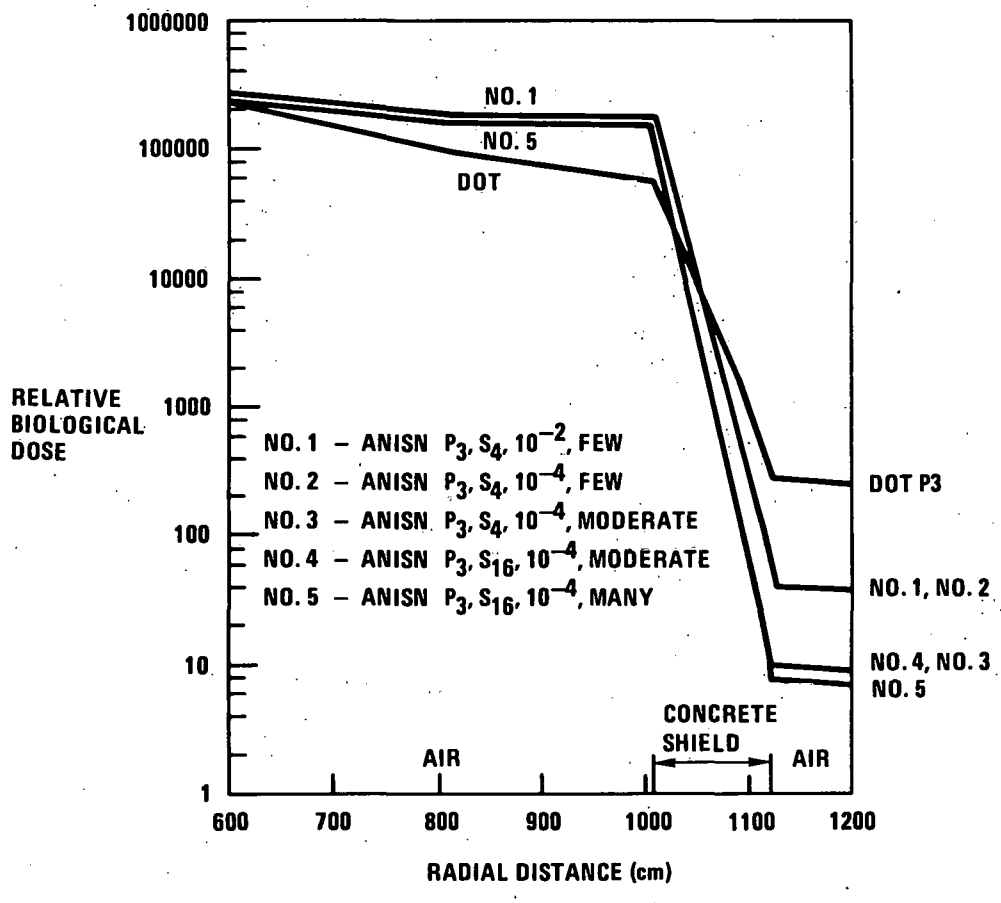

Fig. 22. Relative biological dose versus distance

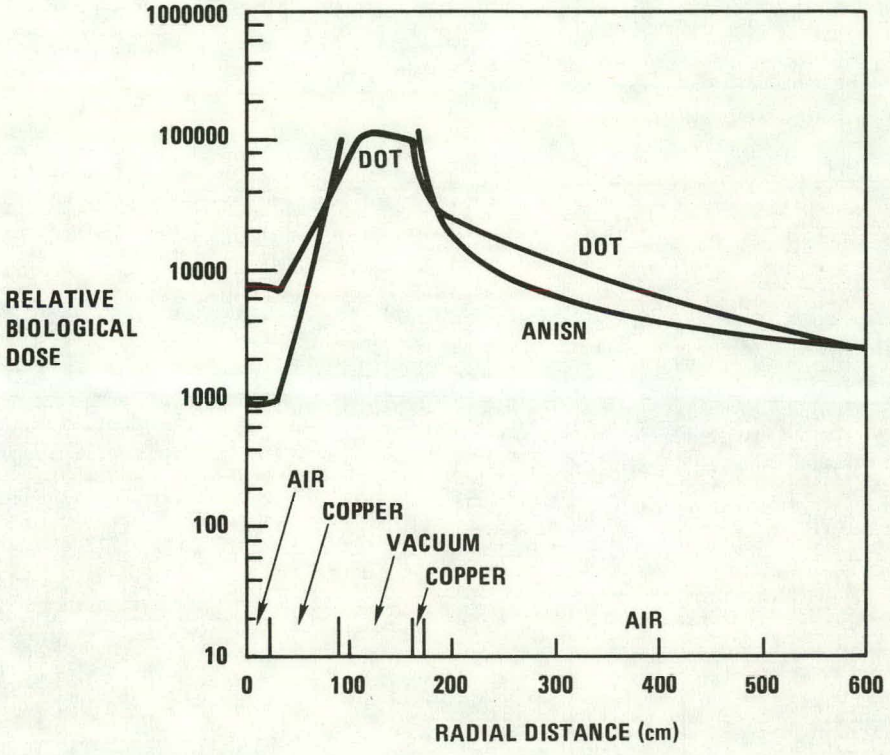

Fig. 23. DOT/ANISN comparison

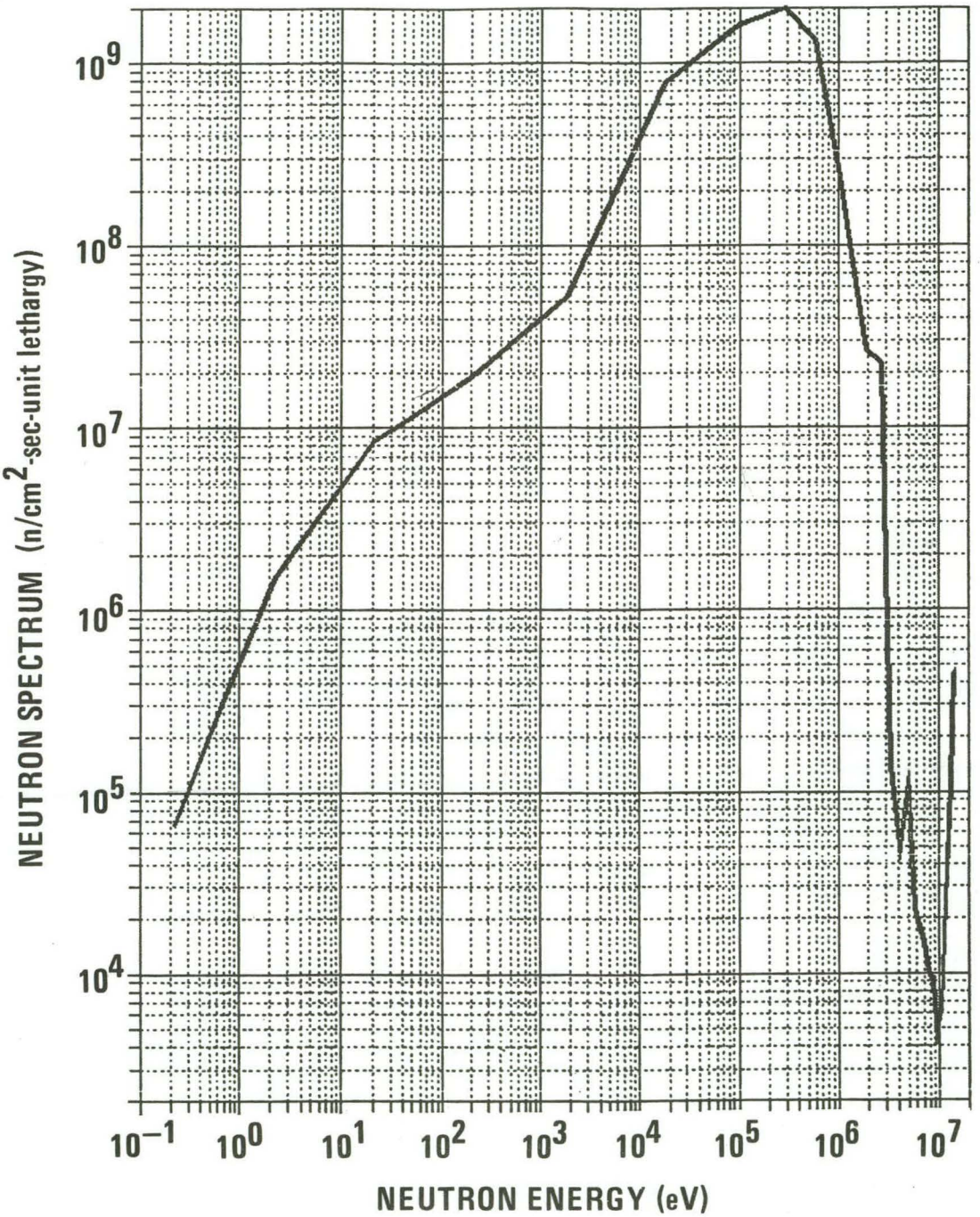

Fig. 24. Neutron spectrum at 0.52 m

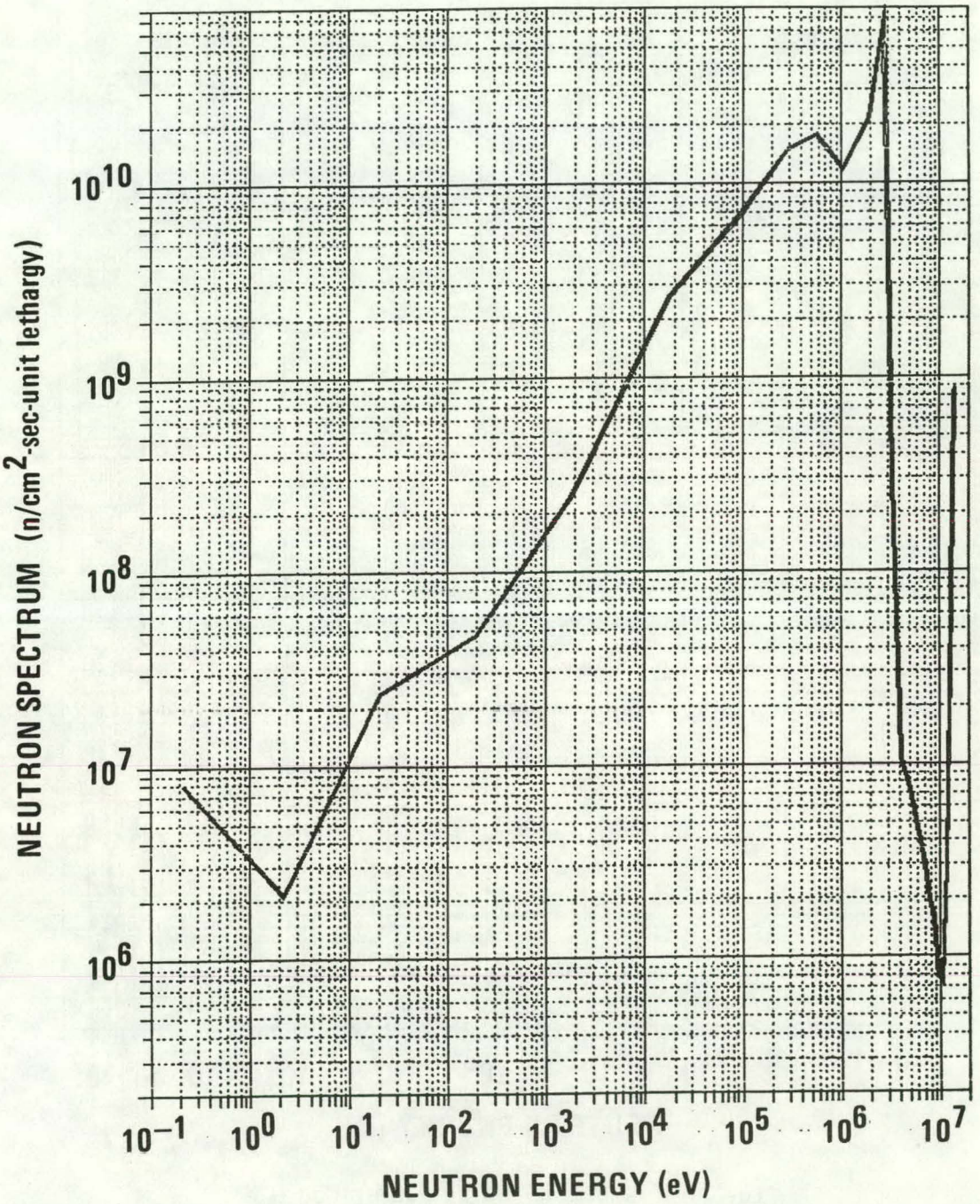

Fig. 25. Neutron spectrum at 1.23 m

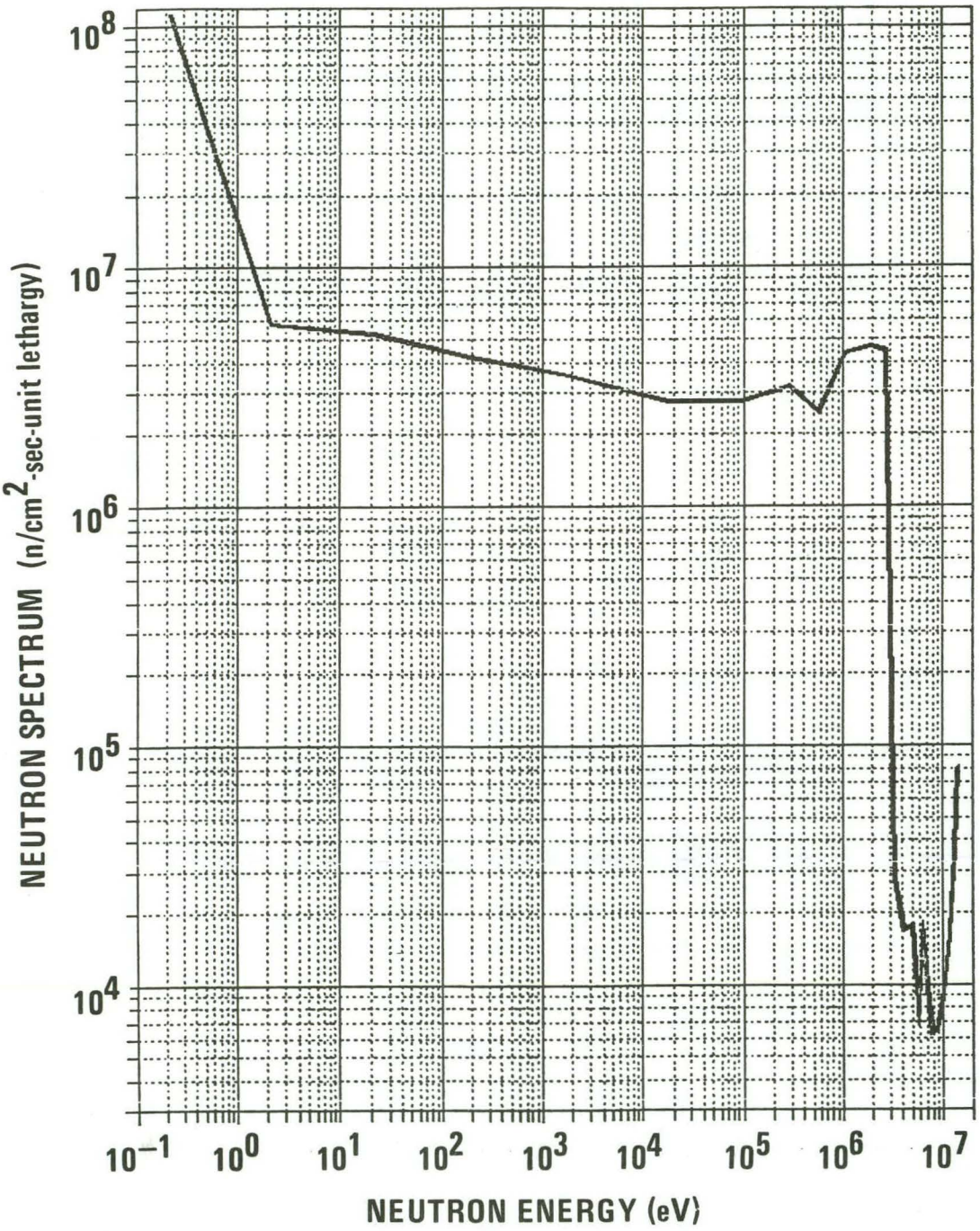

Fig. 26. Neutron spectrum at 10.3 m

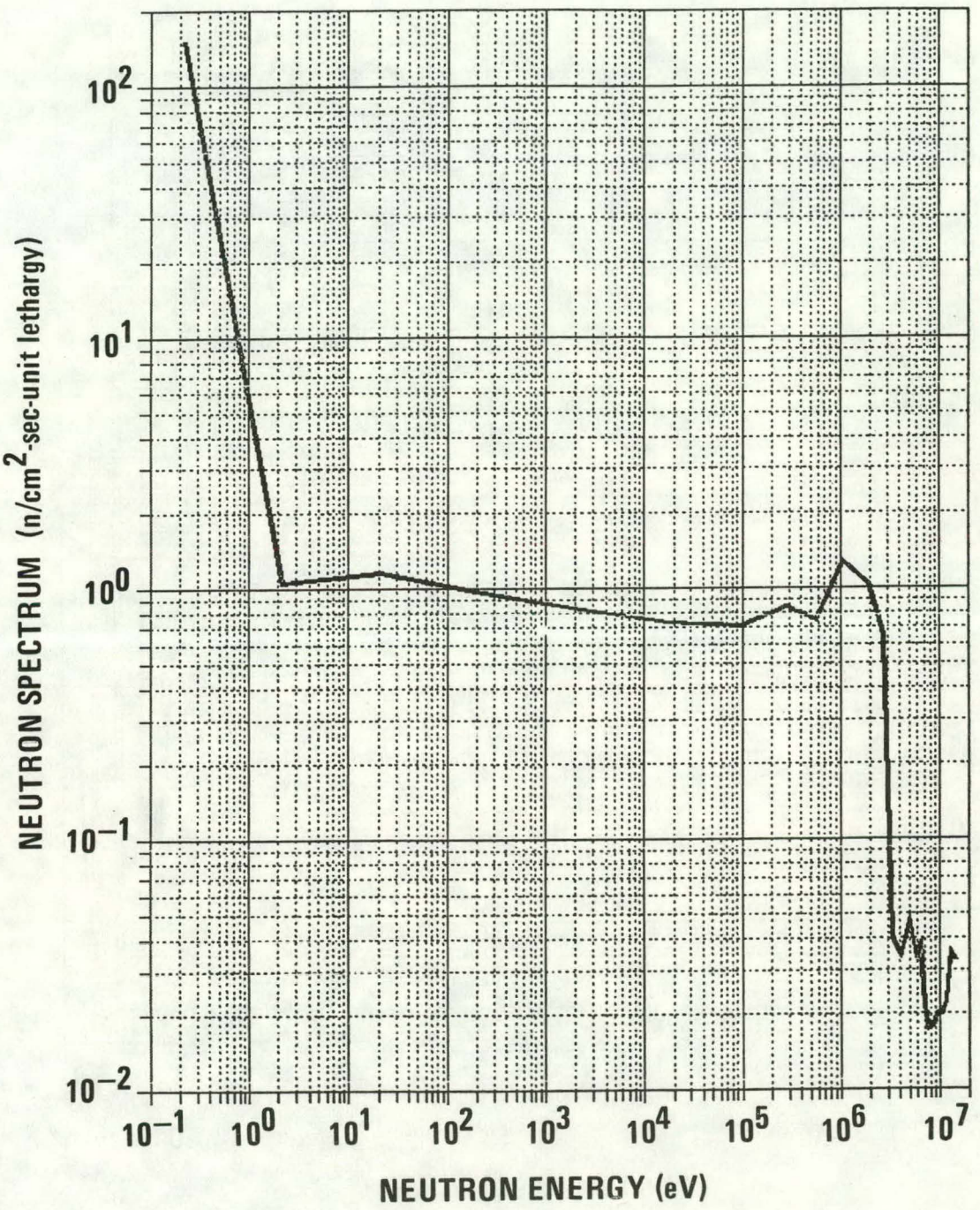

Fig. 27. Neutron spectrum at 127 m

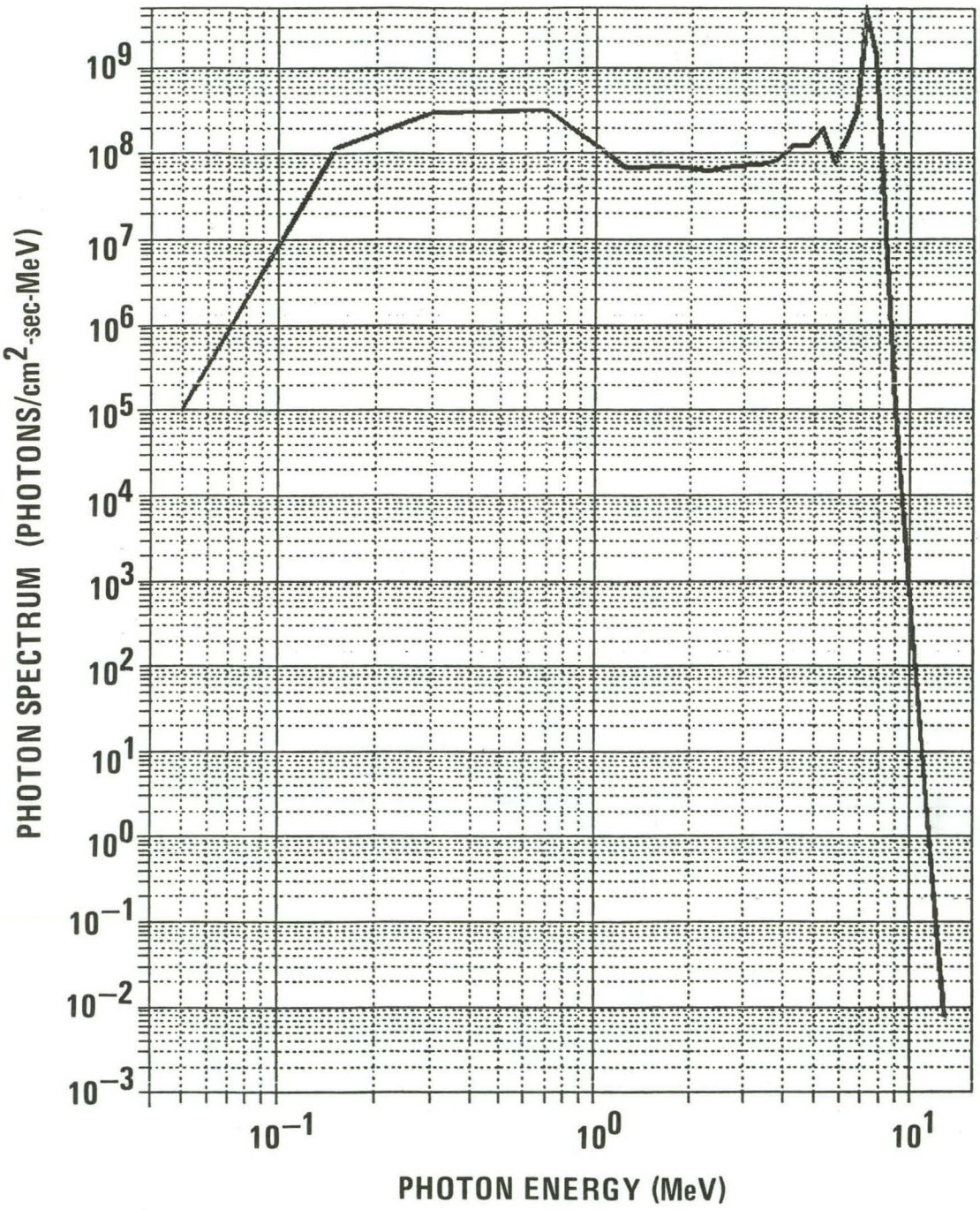

Fig. 28. Photon spectrum at 0.52 m

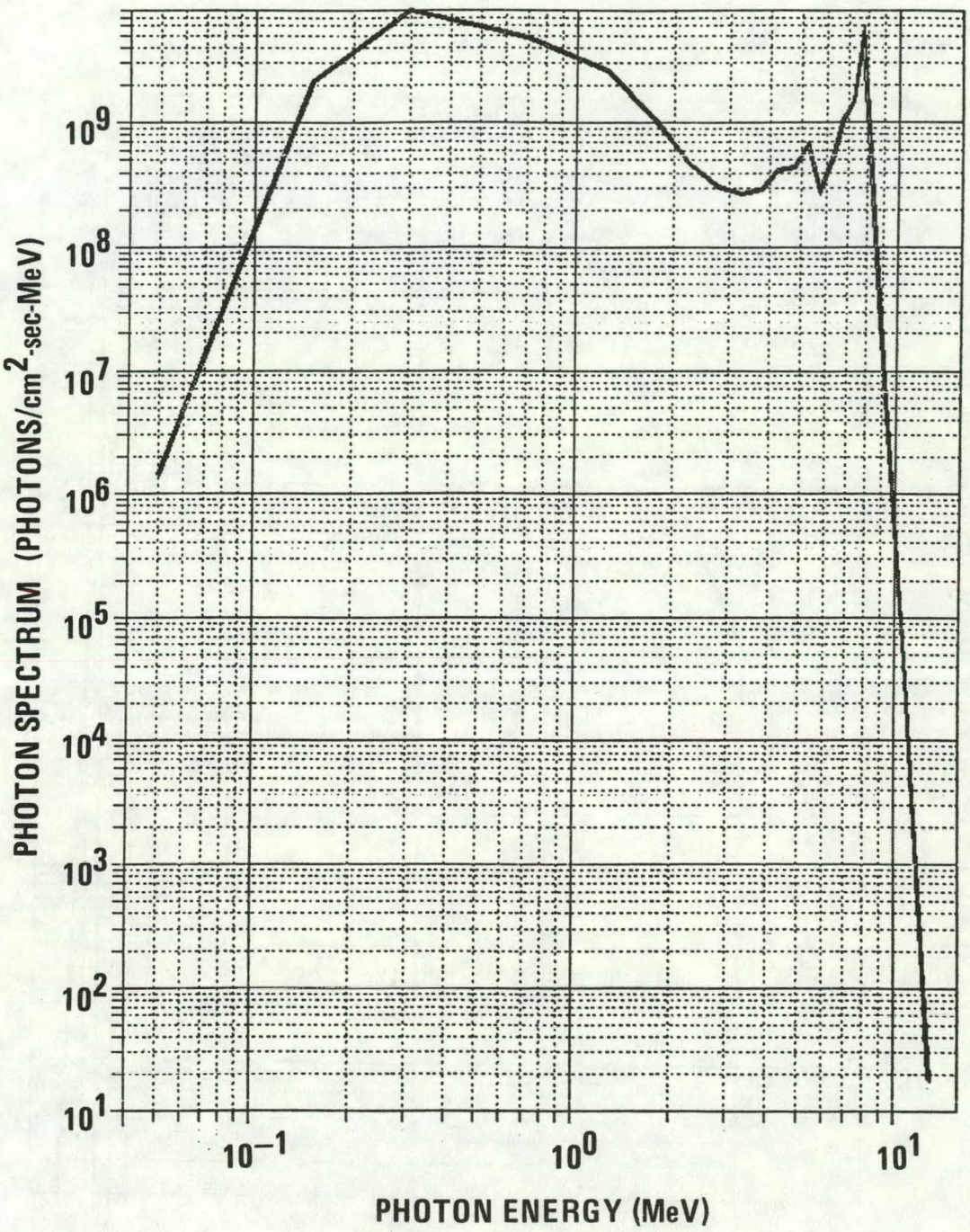

Fig. 29. Photon spectrum at 1.23 m

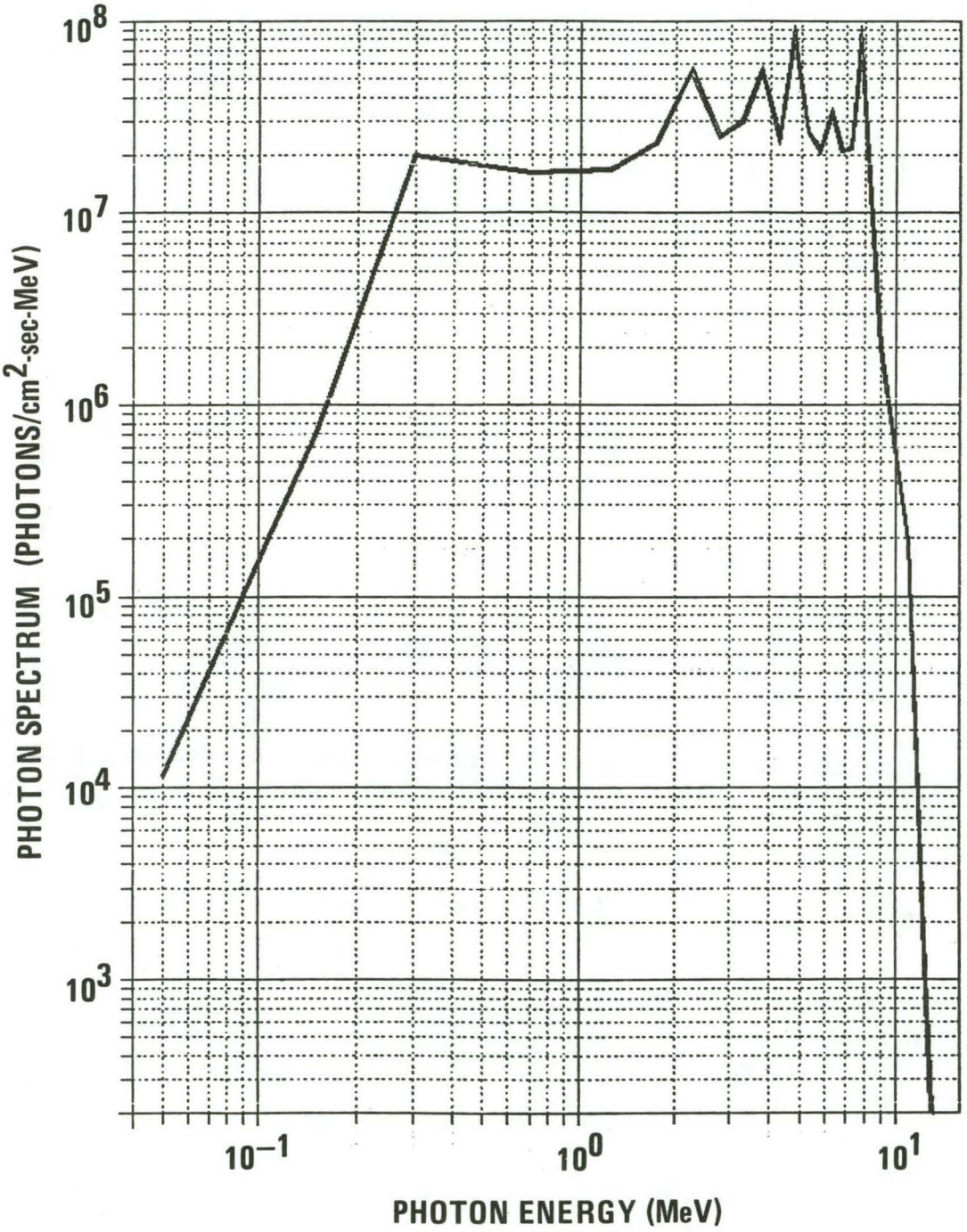

Fig. 30. Photon spectrum at 10.3 m

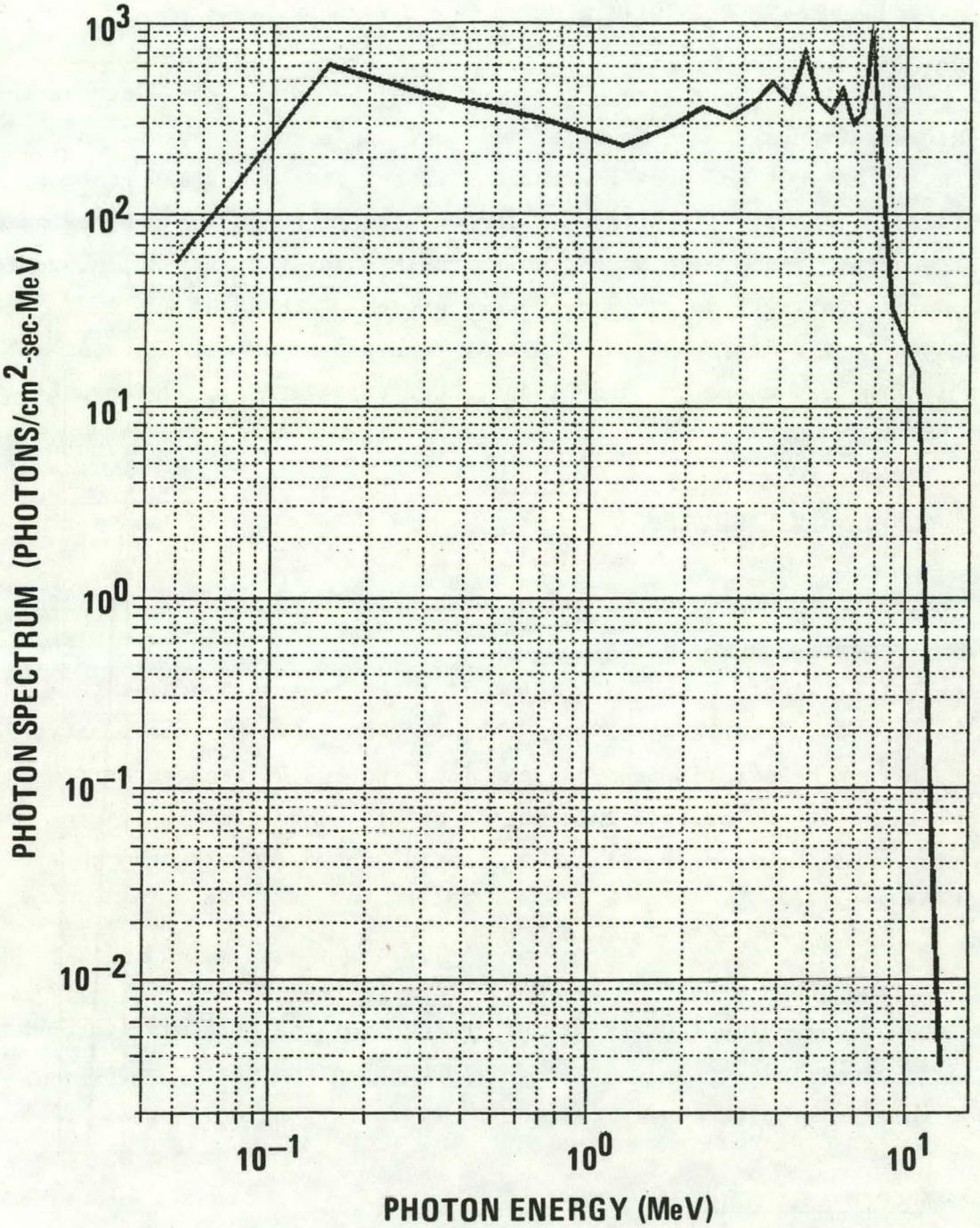

Fig. 31. Photon spectrum at 127 m

4.4. ALBEDO AND STREAMING CALCULATIONS

4.4.1. Neutron Levels in DIII Room

The MUSCAT scattering code[24] was utilized to obtain the distribution of neutron currents in the Doublet III room. This code is based on the view factor concept and requires the assignment of albedos and scattering distributions to all surfaces. The outside of the torus was assigned a fast neutron albedo of 0.4 and an isotropic angular distribution, while the concrete walls, floor, and roof were given an albedo of 0.6 and a cosine scattering distribution. Partial results of the calculation are shown in Fig. 32, where the annual doses correspond to 10,000 Phase II shots per year.

4.4.2. Streaming Estimates

The detailed MUSCAT results were used to resolve several streaming problems, such as shown in Fig. 33, which depicts a penetration of the shield roof by electric conduits for one of the neutral beams. The MUSCAT run showed that about 35% of the neutrons entering this penetration came from below; 15% from the machine; and 50% backscattered from the shield wall. Using this information and standard Simon-Clifford streaming equations resulted in a calculated neutron dose at the power supply of 2 rem/year.

Numerous other streaming estimates of a similar nature were made. While it was generally found difficult to control the streaming through the large electrical conduits, careful layout and the use of concrete shadow shields or pipe chases provided satisfactory solutions.

4.5. INDUCED ACTIVATION

The ANISN runs performed to check the DOT results also provided sufficient data to enable estimates to be made of the shutdown dose rates

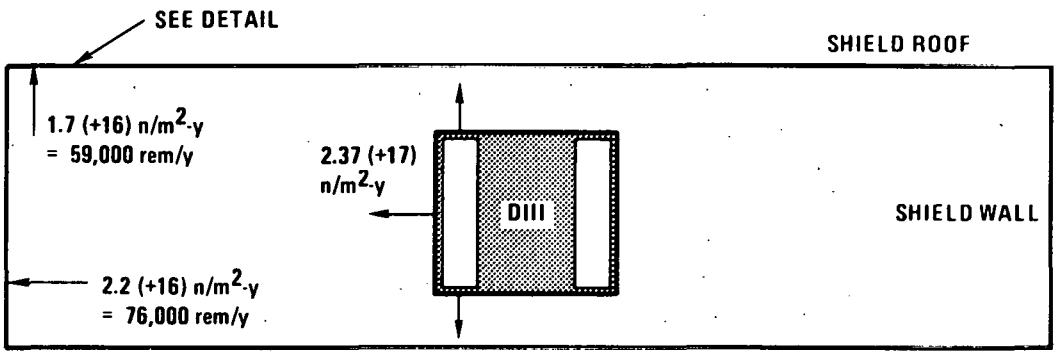

Fig. 32. Neutron doses in DIII room

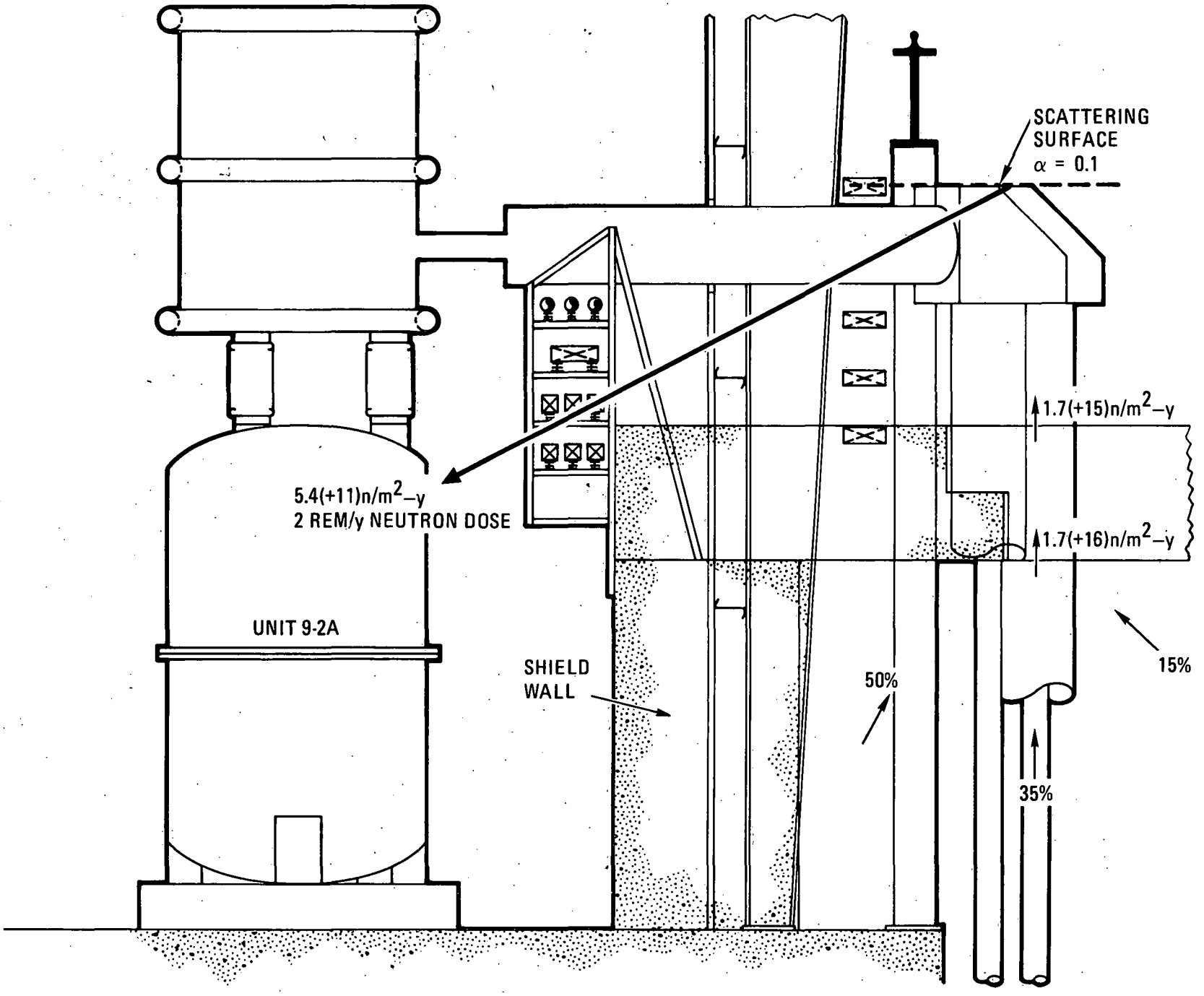

Fig. 33. Streaming detail

in the Inconel plasma chamber. For example, the saturated Cu^{64} activity was found to be 1.5×10^8 disintegrations/cm^3-sec in the copper regions immediately surrounding the plasma chamber. Knowledge of the emission characteristics (1.35 MeV photon 0.6% and 0.51 MeV photon 38%) and elementary shielding theory permitted an estimate of the Cu^{64} shutdown dose rate in the center of the plasma chamber. This and other radionuclide estimates are listed in Table 22.

Table 22

SHUTDOWN DOSE RATE (mrem/hr) IN CENTER OF DIII PLASMA CHAMBER AFTER ONE YEAR D-D OPERATION (10,000 SHOTS PER YEAR, PHASE II)

	Shutdown Time			
	1 hr	12 hrs	1 da	1 wk
Dose rate due to Cu^{64}	28	14.5	7.5	nil
Dose rate due to Co^{58}	2.3	2.3	2.3	2.2
Dose rate due to Mn^{56}	∿8	nil	nil	nil
Total	38	17	10	2

5. REFERENCES

1. T. Ohkawa, "Experimental Objectives and Plans of Doublet III", Trans. Am. Nucl. Soc. 28, 45 (1978).

2. R. A. Grimesey et al., "Preliminary Studies for the PDX Tokamak Radiation Shield Design", TREE-1369, July 1979.

3. C. L. Hsieh, "Possible Features of a Runaway Discharge in Doublet III", General Atomic unpublished data, August 1977.

4. R. A. Lillie et al., "One Dimensional Gamma Ray Shielding Calculations for the EBT-P", Trans. Am. Nucl. Soc. 34, 642 (1980).

5. J. D. Strachan and W. Stodick, "Observations of Runaway Electrons in PLT 400 kA Ohmic Heated Discharges", PPPL, Sept. 1977.

6. B. T. Price, C. C. Horton, and K. T. Spinney, "Radiation Shielding", Pergamon Press, New York, 1957.

7. W. W. Buechner et al., "Thick-Target X-Ray Production in the Range from 1250 to 2350 Kilovolts", Phy. Rev. 74, 10, 1348 (1948).

8. RSIC Computer Code Collection, "AKERN-Aerojet Point Kernel Integration Calculational System", ORNL CCC-190, no date.

9. "Engineering Compendium on Radiation Shielding", Vol. I, Springer-Verlag, 1968, para. 4.5.3.4.

10. "Reactor Handbook - Shielding", Interscience, 1962, Figs. 15.8-15.13.

11. "Neutron Production in Doublet III", General Atomic unpublished data.

12. "Reactor Handbook - Shielding", Interscience, 1962, para. 9.4.

13. ibid., Table 9.9.

14. ibid., Table 9.15.

15. ibid., Fig. 9.22.

16. "Engineering Compendium on Radiation Shielding", Vol. III, Springer-Verlag, 1968, Fig. 10.7-5.

17. "Reactor Handbook - Shielding", Interscience, 1962, Fig. 9.23.

18. ibid., Figs. 15.49-15.57.

19. "Tokamak Fusion Test Reactor Final Design Report", PPPL-1475, August 1978.

20. W. H. Peng and J. Celnik, "Skyshine Analysis for the Intense 14 MeV Neutron Source Facility".

21. A. F. Avery and M. M. Chestnutt, "Shield Design for the Joint European Torus", 5th Int. Conf. on Reac. Sh., 1977.

22. M. E. Battat and D. J. Dudziak, "Shield Analyses for Intense 2.2-pJ (14 MeV) Neutron Sources", 5th Int. Conf. on Reac. Sh., 1977.

23. C. F. Hansen et al, "Radiation Doses as a Function of the Thickness and Shielding Material Surrounding a 14 MeV Neutron Source", 5th Int. Conf. on Reac. Sh., 1977.

24. B. A. Engholm, "The MUSCAT Scattering Code", Nucl. Sci. Eng., 27 (2), 490 (1967).

GENERAL ATOMIC COMPANY
P. O. BOX 81608
SAN DIEGO, CALIFORNIA 92138